Journal of Nuclear Medicine, published on May 19, 2022 as doi:10.2967/jnumed.122.264036

A novel dimeric FAP-targeting small molecule-radio conjugate with high and prolonged tumour uptake

Andrea Galbiati[1,*], Aureliano Zana[1,*], Matilde Bocci[1], Jacopo Millul[1], Abdullah Elsayed[1,2], Jacqueline Mock[1], Dario Neri[2,3†], Samuele Cazzamalli[1†]

[1] Philochem AG, R&D department, CH-8112 Otelfingen, Switzerland;

[2] Swiss Federal Institute of Technology, Department of Chemistry and Applied Biosciences, CH-8093 Zurich, Switzerland;

[3] Philogen S.p.A., 53100 Siena, Italy.

† Corresponding authors:

Dr. Samuele Cazzamalli - Philochem AG, CH-8112 Otelfingen, Switzerland - Phone (+41) 435448800 - samuele.cazzamalli@philochem.ch

Prof. Dr. Dario Neri – Philogen SpA, Philochem AG and ETH Zürich, CH-8112 Otelfingen, Switzerland - Phone (+41) 435448806 - neri@pharma.ethz.ch

*** First authors, contributed equally to this work:**

Dr. Andrea Galbiati – andrea.galbiati@philochem.ch

Aureliano Zana – aureliano.zana@philochem.ch

Philochem AG, CH-8112 Otelfingen, Switzerland - Phone (+41) 435448800

Disclaimer: D.N. is a cofounder and shareholder of Philogen (http://www.philogen.com/en/), a Swiss-Italian Biotech company that operates in the field of ligand-based pharmacodelivery. A.G., A.Z., M.B., J. Millul, A.E., J. Mock and S.C. are employees of Philochem AG, the daughter company of Philogen that owns and has patented OncoFAP (PCT/EP2021/053494) and BiOncoFAP (PCT/EP2022/053404). No other potential conflicts of interest relevant to this article exist.

Short running title: FAP-ligand with prolonged tumour uptake

ABSTRACT:

Imaging procedures based on small molecule-radio conjugates (SMRCs) targeting fibroblast activation protein (FAP) have recently emerged as a powerful tool for the diagnosis of a wide variety of tumours. However, the therapeutic potential of radiolabeled FAP-targeting agents is limited by their short residence time in neoplastic lesions. In this work, we present the development and *in vivo* characterization of BiOncoFAP, a new dimeric FAP-binding motif with extended tumour residence time and favorable tumour-to-organ ratio.

Methods: The binding properties of BiOncoFAP and its monovalent OncoFAP analogue were assayed against recombinant hFAP. Preclinical experiments with ^{177}Lu-OncoFAP-DOTAGA (^{177}Lu-OncoFAP) and ^{177}Lu-BiOncoFAP-DOTAGA (^{177}Lu-BiOncoFAP) were performed in mice bearing FAP-positive HT-1080 tumours.

Results: OncoFAP and BiOncoFAP displayed comparable sub-nanomolar dissociation constants towards hFAP in solution, but the bivalent BiOncoFAP bound more avidly to the target immobilized on solid supports. In a comparative biodistribution study, ^{177}Lu-BiOncoFAP exhibited a more stable and prolonged tumour uptake than ^{177}Lu-OncoFAP (~20% ID/g vs ~4% ID/g, at 24h p.i., respectively). Notably, ^{177}Lu-BiOncoFAP showed favorable tumour-to-organ ratios with low kidney uptake. Both ^{177}Lu-OncoFAP and ^{177}Lu-BiOncoFAP displayed potent anti-tumour efficacy when administered at therapeutic doses in tumour bearing mice.

Conclusions: ^{177}Lu-BiOncoFAP is a promising candidate for radioligand therapy of cancer, with favorable *in vivo* tumour-to-organ ratio, long tumour residence time and potent anti-cancer efficacy.

Keywords: Fibroblast Activation Protein; Theranostics; OncoFAP; Targeted Radiotherapy; Dimeric Targeting Ligands.

INTRODUCTION

Small molecule-radio conjugates (SMRCs) are pharmaceutical products composed of a small organic ligand, acting as tumour targeting agent, and a radionuclide payload, that can be exploited both for diagnostic and therapeutic applications (*1*–*3*). The "theranostic" potential of SMRCs, *id est* the possibility to perform imaging and therapy with the same product, facilitates the clinical development of this new class of drugs (*4*–*7*). Patients who can predictably benefit from targeted radioligand therapy are accurately selected through dosimetry studies (*8*). Lutathera®, a radioligand therapeutic targeting Somatostatin Receptor type 2, is the first SMRC product that gained marketing authorization for the therapy of neuroendocrine tumours (*9*). The use of this drug has consistently shown high response rates and long median progression-free survival in a multicenter phase-III clinical trial (*10*). More recently, a second product named ^{177}Lu-PSMA-617 was shown to provide therapeutic benefit to PSMA-positive metastatic castration-resistant prostate cancer patients in a large phase III clinical trial (*11*). Radioligand therapy with ^{177}Lu-PSMA-617 prolonged imaging-based progression-free survival and overall survival when added to standard care (*11*).

In the last few years, a new category of pan-tumoural tumour-targeting SMRCs specific for Fibroblast Activation Protein (FAP) has been successfully implemented for the diagnosis of solid tumours (*12*–*15*). FAP is a membrane-bound enzyme highly expressed on the surface of cancer-associated fibroblasts in the stroma of more than 90% of human epithelial cancers. FAP expression in healthy tissues is negligible (*12*,*13*,*16*,*17*). We have recently reported the discovery of OncoFAP, the small molecule FAP-targeting agent with the highest affinity reported so far (*18*). Proof-of-concept

targeting studies with ^{68}Ga-OncoFAP-DOTAGA (^{68}Ga-OncoFAP), a PET tracer based on OncoFAP, have confirmed excellent biodistribution in patients with different primary and metastatic solid malignancies (*19*).

Efficacy of radioligand therapeutics is strongly correlated to their residence time in tumoursu (*9*,*20*–*23*). While Lutathera® and PSMA-617 are characterized by a sustained tumour residence time in patients (i.e., ~61 hours for ^{177}Lu-PSMA-617 and ~88 hours for ^{177}Lu-DOTATATE) (*24*,*25*), SMRCs based on FAP-targeting agents are typically cleared from solid lesions in few hours (*26*,*27*). In preclinical biodistribution experiments, ^{177}Lu-OncoFAP selectively localized on neoplastic lesions (~38% ID/g, 1h after systemic administration), but half of the dose delivered to the tumour was lost within 8-12 hours (*18*). A comparable tumour targeting performance and pharmacokinetic profile have been reported for other FAP-targeting SMRCs by Haberkorn and co-workers (e.g., the tumour uptake of ^{177}Lu-FAPI-46 decreased from 12.5% ID/g at 1h to 2.5% ID/g at 24h after administration) (*28*). Importantly, a rapid washout from tumours is observed not only in mice but also in patients treated with ^{177}Lu-FAPI-46 (*26,29*).

In an attempt to extend tumour residence time of FAP-targeting SMRCs and to maximize the exposure of cancer cells to biocidal radiation, we developed BiOncoFAP, a dimeric FAP-targeting OncoFAP-derivative. In this work, we describe the *in vitro* characterization of BiOncoFAP and we report the first preclinical biodistribution and therapy studies with a radiolabeled preparation of this novel dimeric FAP-targeting compound.

MATERIALS AND METHODS

Chemistry and Radiochemistry

(*S*)-4-((4-((2-(2-cyano-4,4-difluoropyrrolidin-1-yl)-2-oxoethyl)carbamoyl)quinolin-8-yl)amino)-4-oxobutanoic acid (named OncoFAP-COOH), OncoFAP-Fluorescein, OncoFAP-Alexa488 and OncoFAP-IRDye750 were synthesized as previously reported by Millul and co-workers (*1*). OncoFAP-DOTAGA (compound 1) and BiOncoFAP-DOTAGA (compound 4) were labeled with cold lutetium by incubation with [^{nat}Lu]$LuCl_3$ in acetate buffer at 90°C for 15 minutes to obtain ^{nat}Lu-OncoFAP-DOTAGA (compound 2) and ^{nat}Lu-BiOncoFAP-DOTAGA (compound 5) which were used as reference compounds for in vitro characterization (inhibition assay and serum stability). Structures of OncoFAP- and BiOncoFAP-conjugates are depicted in Figure 1. Detailed experimental chemical procedures are described in the Supplemental material.

Radiolabeling of OncoFAP-DOTAGA (compound 1) and BiOncoFAP-DOTAGA (compound 4) with lutetium-177 was performed with different specific activities for the different studies (biodistribution and therapy). Prior to the biodistribution study, precursors (compound 1 or 4, 100 nmol) were dissolved in 100 µL of PBS and diluted with 200 µL of sodium acetate (1 M in water, pH = 8). 20 MBq of ^{177}Lu solution were added and the mixture was heated at 90°C for 15 minutes, followed by dilution with 1600 µL of PBS to achieve final volume of 2 mL. Prior to the therapy studies, precursors (compound 1 or 4, 5 nmol) were dissolved in 5 µL of PBS, then sodium acetate buffer (30 µL, 1 M in water) and 15 or 70 MBq of ^{177}Lu solution were added. The mixture was heated at 90°C for 15 minutes followed by dilution with 130 µL of PBS to afford a final volume of 200 µL. Quality control of radiosynthesis was performed using radio-HPLC.

The possibility to form a stable complex between the so obtained ^{177}Lu-radiolabeled derivatives and the target antigen was tested by co-incubating the compounds with recombinant human FAP and loading the mixture onto a desalting PD-10 column run by gravity [Supplemental Figure 1].

In vitro Inhibition Assay on hFAP

Enzymatic activity of hFAP on the Z-Gly-Pro-AMC substrate was measured at room temperature on a microtiter plate reader, monitoring the fluorescence at an excitation wavelength of 360 nm and an emission wavelength of 465 nm. The reaction mixture contained substrate (20 µM), protein (200 pM, constant), assay buffer (50 mM Tris, 100 mM NaCl, and 1 mM EDTA, pH = 7.4), and inhibitors (compounds 1, 2, 4 and 5) with serial dilution from 1.67 µM to 800 fM, 1:2 in a total volume of 20 µL. Experiments were performed in triplicate, and the mean fluorescence values were fitted using Prism 7 (Y = Bottom + (Top − Bottom)/(1 + ((X^HillSlope)/(IC50^HillSlope)))). The value is defined as the concentration of inhibitor required to reduce the enzyme activity by 50% after addition of the substrate [Figure 2].

Affinity Measurement to hFAP by Fluorescence Polarization

Fluorescence polarization experiments were performed in 384-well plates (nonbinding, ps, f-bottom, black, high volume, 30 µL final volume). Stock solutions of proteins were serially diluted (1:2) with buffer (50 mM Tris, 100 mM NaCl, and 1 mM EDTA, pH = 7.4), while the final concentration of the binders (OncoFAP-Fluorescein and BiOncoFAP-Fluorescein) was kept constant at 10 nM. The fluorescence anisotropy was

measured on a Tecan microtiter plate reader. Experiments were performed in triplicate, and the mean anisotropy values were fitted using Prism 7 ((Y = m1 + m2 × 0.5 × ((X + k + m3) − sqrt((X + k + m3)^2 − 4 × X × k)), where k is the concentration of the fluorescent binder). Data are reported in Supplemental Figure 2.

Affinity Measurement to hFAP by Enzyme-Linked Immunosorbent Assay (ELISA)

Recombinant human FAP (1 µM, 5 mL) was biotinylated with Biotin-LC-NHS (100 eq.) by incubation at room temperature under gentle agitation in 50 mM HEPES, 100 mM NaCl buffer (pH=7.4). After 2 hours biotinylated hFAP was purified via PD-10 column and dialyzed overnight in HEPES buffer. The following day a StreptaWell™ (transparent 96-well) was incubated with biotinylated hFAP (100 nM, 100 µL/well) for 1 hour at room temperature and washed with PBS (3x, 200 µL/well). The protein was blocked by adding 4% Milk in PBS (200 µL/well, 30 min at RT) and then washed with PBS (3x, 200 µL/well). Immobilized hFAP was incubated for 30 minutes in the dark with serial dilutions of OncoFAP-Fluorescein (compound 7) and BiOncoFAP-Fluorescein (compound 8), then washed with PBS (3x, 200 µL/well). A solution of rabbit αFITC antibody (1 µg/mL, Bio-Rad 4510-7804) in 2% Milk-PBS was added to each well (100 µL/well) and incubated for additional 30 minutes in the dark. The resulting complex was washed with PBS (3x, 200 µL/well) and incubated for additional 30 minutes of protein A-HRP (1 µg/mL in 2% Milk-PBS, 100 µL/well). Each well was washed with PBS 0.1% Tween (3x, 200 µL/well) and with PBS (3x, 200 µL/well). The substrate (TMB - 3,3',5,5'-Tetramethylbenzidine) was added (100 µL/well) and developed in the dark for 2

minutes. The reaction was stopped by adding 50 µL of 1M sulphuric acid. The absorbance was measured at 450 nm (ref 620-650 nm) with a TECAN spark

Internalization Studies by Confocal Microscopy Analysis

SK-RC-52.hFAP and HT-1080.hFAP cells were seeded into 4-well coverslip chamber plates (Sarstedt, Inc.) at a density of 10^4 cells per well in RPMI or DMEM medium, respectively (1 mL, Invitrogen) supplemented with 10% Fetal Bovine Serum (FBS, Gibco), Antibiotic-Antimytotic (Gibco), and 10 mM HEPES (VWR). Cells were allowed to grow overnight under standard culture conditions. The culture medium was replaced with fresh medium containing the suitable Alexa488-conjugated probes (100 nM) and Hoechst 33342 nuclear dye (Invitrogen, 1 µg/mL). Colonies were randomly selected and imaged 30 min after incubation on a SP8 confocal microscope equipped with an AOBS device (Leica Microsystems) [Figure 3].

Animal Studies

All animal experiments were conducted in accordance with Swiss animal welfare laws and regulations under the license number ZH006/2021 granted by the Veterinäramt des Kantons Zürich.

Implantation of Subcutaneous Tumours

Tumour cells were grown to 80% confluence in Dulbecco's Modified Eagle Medium (DMEM, Gibco) or RPMI-1640 (Gibco) with 10% fetal bovine serum (FBS) (Gibco) and 1% antibiotic-antimycotic (Gibco) and detached with Trypsin-EDTA

(ethylenediaminetetraacetic acid) 0.05%. Tumour cells were resuspended in Hanks' Balanced Salt Solution medium. Aliquots of 5×10^6 cells (100 µL of suspension) were injected subcutaneously in the flank of female athymic Balb/c AnNRj-Foxn1 mice (6 to 8 wk of age, Janvier).

Quantitative Biodistribution of ^{177}Lu-OncoFAP and ^{177}Lu-BiOncoFAP in Tumour-Bearing Mice

OncoFAP-DOTAGA (compound 1) and BiOncoFAP-DOTAGA (compound 4) were radiolabeled with ^{177}Lu (as described in the Supplemental material). Tumours were allowed to grow to an average volume of 500 mm^3. Mice were randomized (n = 4/5 per group) and injected intravenously with radiolabeled preparations of ^{177}Lu-OncoFAP and ^{177}Lu-BiOncoFAP (250 nmol/kg; 50 MBq/kg). Mice were euthanized at different time-points (1h, 4h, 17h and 24h) after the intravenous injection by CO_2 asphyxiation. Tumours, organs, and blood were harvested, weighted, and radioactivity was measured with a Packard Cobra Gamma Counter. Values are expressed as percent ID/g ± SD [Figure 4]. The %ID/g in the tumours was corrected by tumour growth rate (*30*).

Therapy Studies with ^{177}Lu-OncoFAP and ^{177}Lu-BiOncoFAP in Tumour-Bearing Mice

The anti-cancer efficacy of ^{177}Lu-OncoFAP and ^{177}Lu-BiOncoFAP was assessed in athymic Balb/c AnNRj-Foxn1 mice bearing HT-1080.hFAP (right flank) and HT-1080.wt (wild type, left flank). ^{177}Lu-OncoFAP or ^{177}Lu-BiOncoFAP were intravenously administered at a dose of 250 nmol/kg, with 15 or 70 MBq/mouse (single administration,

following the schedule indicated in Figure 5). Therapy experiments started when the average volume of established tumours had reached 100-150 mm^3. Body weight of the animals and tumour volume were daily measured and recorded. Tumour dimensions were measured with an electronic caliper and tumour volume was calculated with the formula (long side, mm) × (short side, mm) × (short side, mm) × 0.5. Animals were euthanized when one or more termination criterium indicated by the experimental license was reached (e.g., weight loss > 15%). Prism 7 software (GraphPad Software) was used for data analysis.

RESULTS

Preparation of OncoFAP and BiOncoFAP Conjugates

The dimeric ligand (BiOncoFAP-COOH, compound 13) was chemically synthesized exploiting L-Lysine for the multimerization of the OncoFAP targeting moiety. The free carboxylic acid served as functional group for the conjugation of fluorophores (BiOncoFAP-Fluorescein 8, BiOncoFAP-Alexa488 10 and BiOncoFAP-IRDye750 12) and of DOTAGA chelator (compound 4). All compounds were produced in high yields and purities [Supplemental material]. Monovalent OncoFAP and corresponding conjugates (OncoFAP-Fluorescein 7, OncoFAP-Alexa488 9 and OncoFAP-IRDye750 11) were synthesized following established procedures (*18*). Chemical structures of OncoFAP and BiOncoFAP derivatives are illustrated in Figure 1 and in Supplemental material. Radiolabeling of OncoFAP-DOTAGA (compound 1) and BiOncoFAP-DOTAGA (compound 4) with ^{177}Lu was achieved in high yield and purity [Supplemental material]. After radiolabeling, ^{177}Lu-OncoFAP and ^{177}Lu-BiOncoFAP retained the ability to form stable complexes with recombinant human FAP, as assessed by PD-10 co-elution experiment. Both compounds are highly hydrophilic, with experimental Log$D_{7.4}$ values of – 4.02 ± 0.22 (n = 5) and – 3.60 ± 0.31 (n = 5), respectively [Supplemental material].

In Vitro Inhibition Assay Against hFAP

We evaluated the inhibitory activity of OncoFAP-DOTAGA (1), BiOncoFAP-DOTAGA (compound 4) and their ^{nat}Lu cold-labeled derivatives (compounds 2 and 5, respectively) against human recombinant FAP (hFAP). Compounds 4 and 5 displayed enhanced inhibitory activity against the target (IC_{50} = 168 and 192 pM, respectively)

compared to their monovalent counterparts (OncoFAP-DOTAGA IC_{50} = 399 pM, ^{nat}Lu-OncoFAP-DOTAGA IC_{50} = 456 pM) [Figure 2A and 2B].

Assessment of Binding Properties of BiOncoFAP to Soluble and Immobilized Human Recombinant Fibroblast Activation Protein

In order to study the binding properties of OncoFAP and BiOncoFAP to soluble hFAP, we measured the affinity constant (K_D) of the corresponding fluorescein conjugates (compound 8, OncoFAP-Fluorescein and compound 9, BiOncoFAP-Fluorescein) in Fluorescence Polarization assays [Figure 2C]. Compounds 8 and 9 exhibited comparable sub-nanomolar K_D values against hFAP (respectively 795 and 781 pM). Moreover, both compounds showed to be very selective for FAP and did not bind to a set of non-target proteins up to micromolar concentrations [Supplemental Figure 2]. Our data confirms that the dimerization does not impair the affinity and selectivity of BiOncoFAP for its target. Then, we studied the binding affinity to hFAP immobilized on a solid support of the dimeric ligand. In a comparative ELISA, BiOncoFAP-Fluorescein exhibited a lower K_D compared to OncoFAP-Fluorescein (8.60 nM vs 32.3 nM, respectively) [Figure 2B and 2D].

Confocal Microscopy Analysis on Tumour Cells

Binding of BiOncoFAP to FAP-positive SK-RC-52 and HT-1080 cancer cells and internalization were assessed by confocal microscopy analysis using the corresponding Alexa-488 conjugate (compound 10). OncoFAP-Alexa488 (compound 9) was used in the same experiment positive control, while untargeted analogues were included as

non-binding negative controls [chemical structures are depicted in the Supplemental material]. OncoFAP and BiOncoFAP displayed comparable binding features on living tumour cells. Both compounds showed lack of internalization on FAP-positive SK-RC-52 cells, while high membrane trafficking was observed when compounds were incubated on HT-1080.hFAP cells [Figure 3].

Stability Studies

The stability of cold-labeled ^{nat}Lu-BiOncoFAP-DOTAGA was assessed in human and mouse serum after incubation at 37°C for 24, 48, 72 and 120 hours. The test compound exhibited half-life longer than 5 days in all experimental conditions. No loss of lutetium (^{nat}Lu) from the DOTAGA chelator was detected [Supplemental Figure 3].

Biodistribution of OncoFAP and BiOncoFAP in Tumour-Bearing Mice

Qualitative biodistribution of OncoFAP and BiOncoFAP was assessed in tumour-bearing mice using a near-infrared fluorophore (IRDye750) as detection agent. Macroscopic imaging of mice implanted with SK-RC-52.hFAP (right flank) and SK-RC-52.wt (left flank) tumours revealed that both OncoFAP-IRDye750 (compound 11) and BiOncoFAP-IRDye750 (compound 12) selectively accumulated in FAP-positive tumours [Supplemental Figures 4 and 5]. Interestingly, BiOncoFAP-IRDye750 conjugate exhibited a longer residence time at the site of disease. Encouraged by these results, we studied the quantitative biodistribution of ^{177}Lu-BiOncoFAP in athymic Balb/c mice bearing HT-1080.hFAP (right flank) and HT-1080.wt (left flank) tumours. A direct comparison with ^{177}Lu-OncoFAP was included in the experiment [Figure 4]. Both

compounds accumulated selectively in FAP-positive tumours shortly after intravenous administration. The dimeric ^{177}Lu-BiOncoFAP product exhibited a more stable and prolonged tumour uptake as compared to its monovalent counterpart (~20% ID/g vs ~4% ID/g, 24h after systemic administration). Notably, ^{177}Lu-BiOncoFAP did not show significant uptake in healthy organs, with favorable tumour-to-organ ratio (e.g., 22-to-1 tumour-to-kidney and 70-to-1 tumour-to-liver ratio, at the 48 h time point) [Supplemental Tables 1-4].

In vitro Cell Binding and Efflux Assays with ^{177}Lu-OncoFAP and ^{177}Lu-BiOncoFAP on HT-1080.hFAP cells

Cell binding of ^{177}Lu-OncoFAP and ^{177}Lu-BiOncoFAP was assessed on HT-1080.hFAP cells, following literature procedures (*29*). Both compounds showed high binding properties towards the FAP-positive cell line. The binding was efficiently antagonized by large excess of “cold” competitors (OncoFAP-DOTAGA or BiOncoFAP-DOTAGA) [Supplemental Figure 6A]. Cell efflux experiments revealed a longer $t_{1/2}$ for ^{177}Lu-BiOncoFAP (~36 h) compared to the monovalent counterpart (~18 h) [Supplemental Figure 6B].

Therapy Study

Therapeutic efficacy of ^{177}Lu-OncoFAP and of ^{177}Lu-BiOncoFAP was assessed in mice bearing HT-1080.hFAP tumours on the right flank and HT-1080.wt tumours on the left flank [Figure 5 and Supplemental Figure 7]. Systemic administration of both compounds at therapeutic doses (15 or 70 MBq/mouse, 250 nmol/Kg) resulted in

selective and potent anti-cancer activity against the growth of HT-1080.hFAP as compared to mice injected with saline. The most active compound in our therapy studies was ^{177}Lu-BiOncoFAP. Tumour growth of FAP-negative lesions (HT-1080.wt) was not influenced by the treatment with ^{177}Lu-OncoFAP and with ^{177}Lu-BiOncoFAP. No significant change in mice body weight was detected both at 15 MBq and at 70 MBq doses [Supplemental Figure 8].

DISCUSSION

FAP-targeted radiopharmaceuticals may revolutionize the field of radioligand imaging of cancer, because of their applicability to many types of malignancies and for the excellent tumour selectivity which has already been proven at the clinical level (*12*,*13*,*19*). Other SMRC products, ^{177}Lu-PSMA-617 and Lutathera®, are limited to certain specific cancer indications and may be taken up by certain normal organ structures (*31*,*32*). FAP is mainly expressed in the stroma of solid malignancies and on the tumour cell surface of mesenchymal tumours, thus adding a new element of differentiation compared to previously established targeting platforms, based on Somatostatin Receptor type 2 and PSMA (*12*,*13*,*16*,*17*) that are expressed on the surface of cancer cells. In this context, accurate selection of the radionuclide payload is crucial for the success of FAP-targeted radiotherapy. While alpha-emitters are characterized by a short range, typically >100 μm (*33*) which may be insufficient, the use of a beta-emitter radionuclide such as ^{177}Lu (path length of ~1.5 mm) (*33*) may enable the killing of stromal cells and surrounding tumour cells (*34*,*35*).

Sustained accumulation of SMRCs in tumours is fundamental for the effective delivery of high radiation doses over time at the site of disease, and therefore for the success of the therapeutic treatment. Among different approaches employed in the past, the dimerization of high affinity ligands has been proposed as a strategy to enhance residence time in antigen-positive structures (i.e., in FAP-positive tumours) (*23*,*36*–*39*). Dimeric ligands present higher chances of re-binding to their target, with slower off-rates as compared to their monovalent counterparts (*40*). However, increase in the binding valency typically leads to higher uptake in healthy tissues (*21*,*38*,*39*). To

the best of our knowledge, three dimeric FAP-targeting radionuclides named DOTA/DOTAGA.(SA.FAPi)$_2$ (*41*,*42*), DOTA-2P(FAPi)$_2$ (*21*) and ND-bisFAPI (*29*) have recently been described. While preclinical biodistribution data are not available for DOTA/DOTAGA.(SA.FAPi)$_2$, DOTA-2P(FAPi)$_2$ was extensively characterized in HCC-PDX-1 mouse model. Despite its slightly increased tumour uptake compared to the monovalent FAPi-46 (~9% vs ~4% ID/g 1h p.i.), the dimeric ligand presents low tumour-to-organ ratios both at 1 and 4h, with a particular liability for the kidney (~1.2-to-1 and ~1.5-to-1 tumour-to-kidney ratio, respectively) (*21*). Similarly, ND-bisFAPI exhibited increased tumor uptake in A549-FAP xenografts, with low tumour-to-organ ratios at all the investigated time-points (i.e., from 1 h to 72 h after systemic administration) (*29*). BiOncoFAP, the novel homodimeric FAP-targeting small organic ligand described in this article, shows specific and persistent tumour uptake (~30% ID/g 1 h p.i. and ~16% ID/g, 48 h p.i.) in HT-1080.hFAP tumour bearing mice. Remarkably, ^{177}Lu-BiOncoFAP presents a clean preclinical biodistribution profile with high tumour-to-organ ratios even at early time-points (e.g., ~7-to-1 and ~10-to-1 tumour-to-kidney, and ~20-to-1 and ~34-to-1 tumour-to-liver ratio, at the 1h and 4h time points, respectively).

The *in vivo* anti-cancer activity of ^{177}Lu-FAPI-46 (beta-emitter) and ^{225}Ac-FAPI-46 (alpha-emitter) has been recently evaluated in PANC-1 tumour bearing mice, a xenograft model of pancreatic cancer characterized by high stromal expression of FAP (*35*). Both products showed only a limited tumour growth suppression even at the highest dose (i.e., 30 kBq/mouse for ^{225}Ac-FAPI-46 and 30 MBq/mouse for ^{177}Lu-FAPI-46).

Collectively, our biodistribution and therapy results show that both ^{177}Lu-OncoFAP and ^{177}Lu-BiOncoFAP are able to efficiently localize at the tumour site and produce potent anti-cancer effect in mice bearing subcutaneous FAP-positive tumours, after a single administration at a dose of 70 MBq/mouse (~2 mCi/mouse) or 15 MBq (~0.4 mCi/mouse). Compared to the monomeric ^{177}Lu-OncoFAP, our new bivalent ^{177}Lu-BiOncoFAP displayed an enhanced *in vivo* anti-tumour activity. As expected, lack of tumour suppression was observed for the FAP-negative tumours (HT-1080.wt), which were used as internal control to appreciate the specificity of OncoFAP-based theranostic products towards FAP-positive solid lesions. In this article, we present favorable biodistribution profile and therapeutic efficacy of ^{177}Lu-OncoFAP and ^{177}Lu-BiOncoFAP obtained in xenograft models with stable homogeneous expression of hFAP on the surface of tumor cells. Further investigations in tumor models with a stromal pattern of FAP expression (e.g., Patients-Derived Xenografts) will be of pivotal importance to predict the therapeutic performance of OncoFAP and BiOncoFAP-based therapeutics in the view of future clinical studies.

Considering exquisite selectivity for cancer lesions and pan-tumoural properties of FAP-target radioligand therapeutics, this new class of radiopharmaceutical products may represent a breakthrough in cancer therapy (*12*). Interim reports on the efficacy of FAP-targeting peptides and small organic ligands developed so far have shown limitation of this therapeutic strategy (*26*,*43*). Escalation of the dose of radiolabeled FAP-targeting peptides is limited by their intrinsically high kidney uptake at late time-points (*43–45*). Therapy with small organic ligands based on FAPI-46 may be limited by their short residence time in the tumour (*26*,*46*). We have developed ^{177}Lu-BiOncoFAP,

a new radioligand therapeutic product with prolonged *in vivo* tumour uptake, and highly favorable tumour-to-kidney ratios. Future clinical studies in a basket of indications will provide clarity on the therapeutic efficacy of this novel FAP-targeted product.

CONCLUSION

^{177}Lu-BiOncoFAP is a promising FAP-targeted SMRC product for tumour therapy. This novel bivalent FAP-targeted compound binds its target with high affinity and shows long residence time in tumour lesions, with favorable tumour-to-organ ratios. Once administered at therapeutic doses, ^{177}Lu-BiOncoFAP potently inhibits growth of FAP-positive tumours in mice. Our data support clinical development of ^{177}Lu-BiOncoFAP in the frame of targeted radioligand therapy.

ACKNOWLEDGEMENTS

The authors would like to thank Ettore Gilardoni for performing exact mass analysis of compounds presented in this article, and Frederik Peissert and Luca Prati for their support with small molecule-ELISA experiments.

Availability of data and material

Additional data is available in the Supplement Material

KEY POINTS

QUESTION: Does ligand dimerization enhance tumor retention time and therapeutic potential of FAP targeting radio-conjugates?

PERTINENT FINDINGS: Compared to the OncoFAP monovalent counterpart, the dimeric ^{177}Lu-BiOncoFAP shows a higher and prolonged tumor uptake in tumor-bearing mice. ^{177}Lu-BiOncoFAP displays a potent *in vivo* anti-cancer effect in preclinical murine models.

IMPLICATIONS FOR PATIENT CARE: The prolonged tumor uptake of ^{177}Lu-BiOncoFAP supports clinical development for the targeted radioligand therapy of multiple FAP-positive cancer lesions.

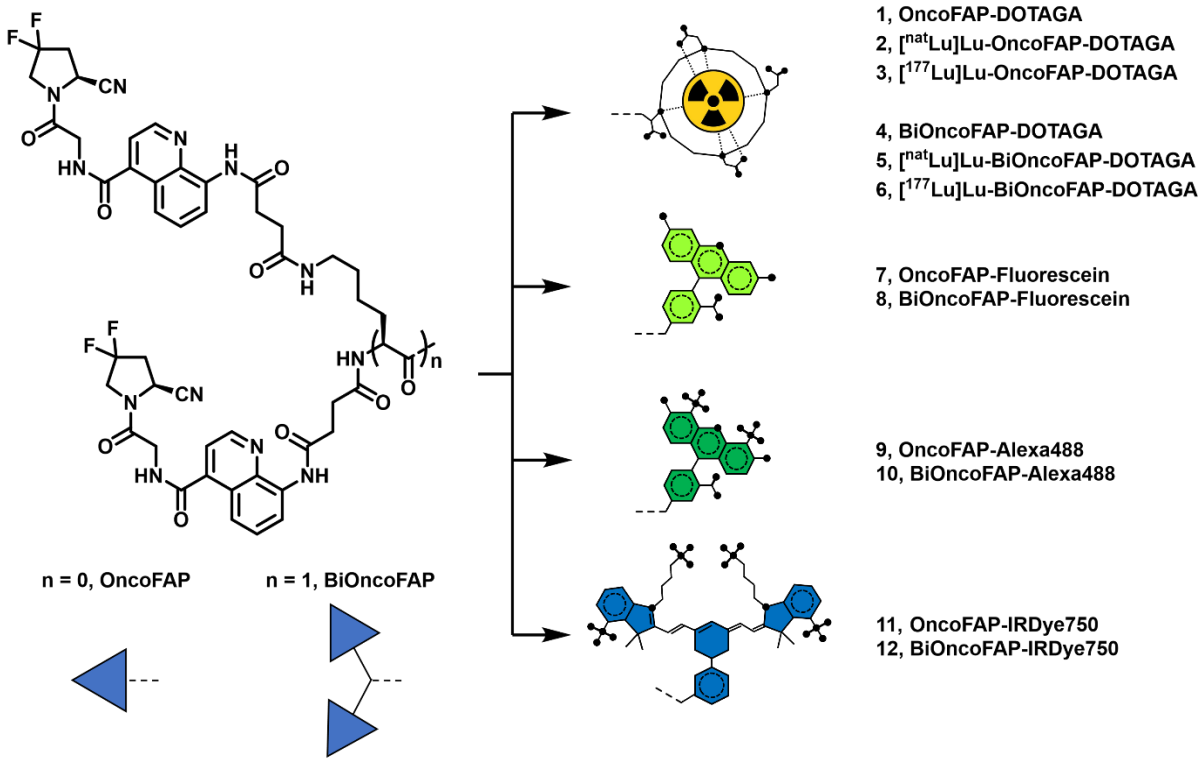

Figure 1. Chemical structures of OncoFAP and BiOncoFAP conjugates (schemes). BiOncoFAP and OncoFAP and their DOTAGA, Fluorescein, Alexa488 and IRDye750 conjugates are presented.

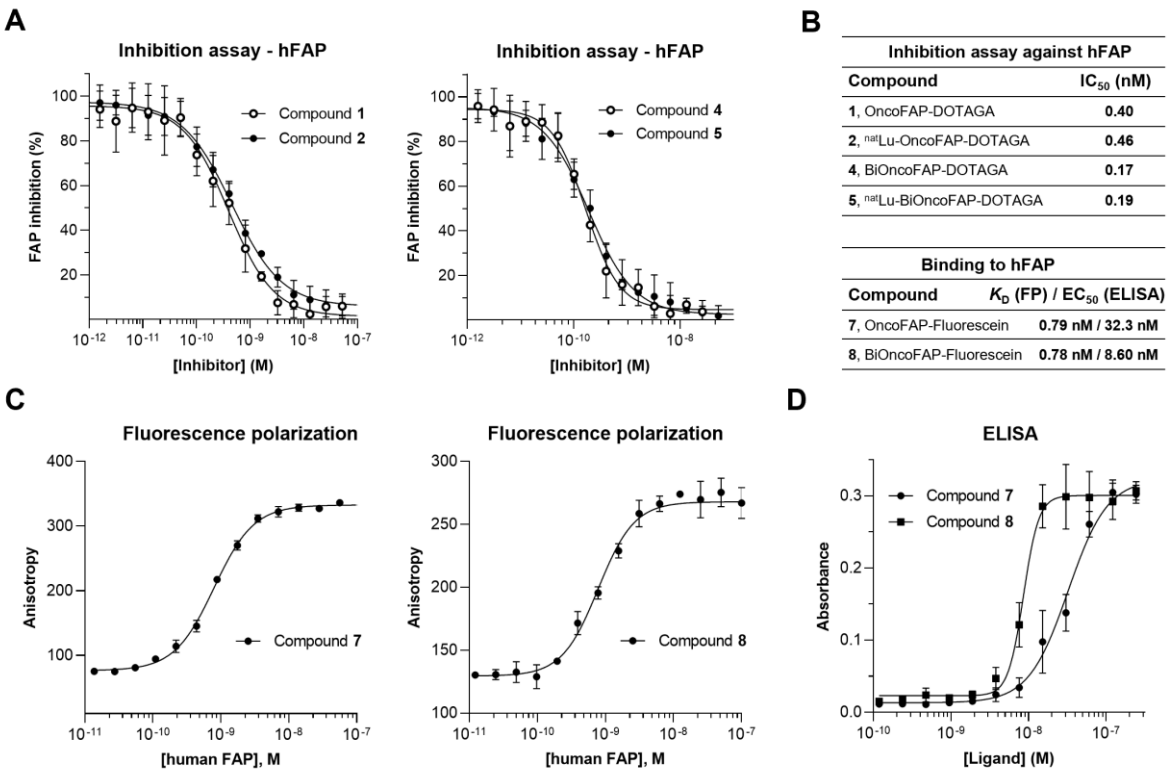

Figure 2. Enzymatic assays performed with (*A*) OncoFAP-DOTAGA (compound 1), BiOncoFAP-DOTAGA (compound 2), and their corresponding cold ^{nat}Lu-labeled derivatives (compounds 2 and 5). *(B)* Binding affinity and IC_{50} values of OncoFAP and BiOncoFAP derivatives towards hFAP. Affinity measurement of (*C*) OncoFAP-Fluorescein (compound 7) and BiOncoFAP-Fluorescein (compound 8) to recombinant human Fibroblast Activation Protein by fluorescence polarization. Both compounds showed ultra-high affinity for the FAP target. (*D*) ELISA experiment on OncoFAP-Fluorescein (compound 7) and BiOncoFAP-Fluorescein (compound 8) against hFAP.

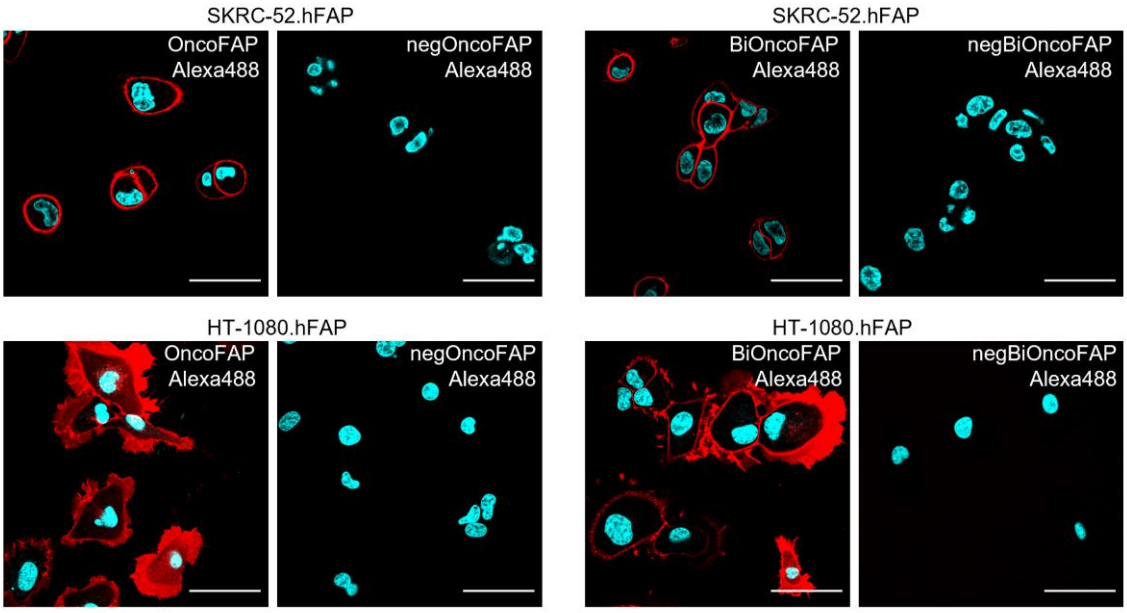

Figure 3. Confocal microscopy images after incubation of OncoFAP-Alexa488 (compound 9) and BiOncoFAP-Alexa488 (compound 10) with SK-RC-52.hFAP or HT-1080.hFAP. Red = fluorescein derivatives staining; blue = Hoechst 33342 staining. (Scale bar = 50 µm.).

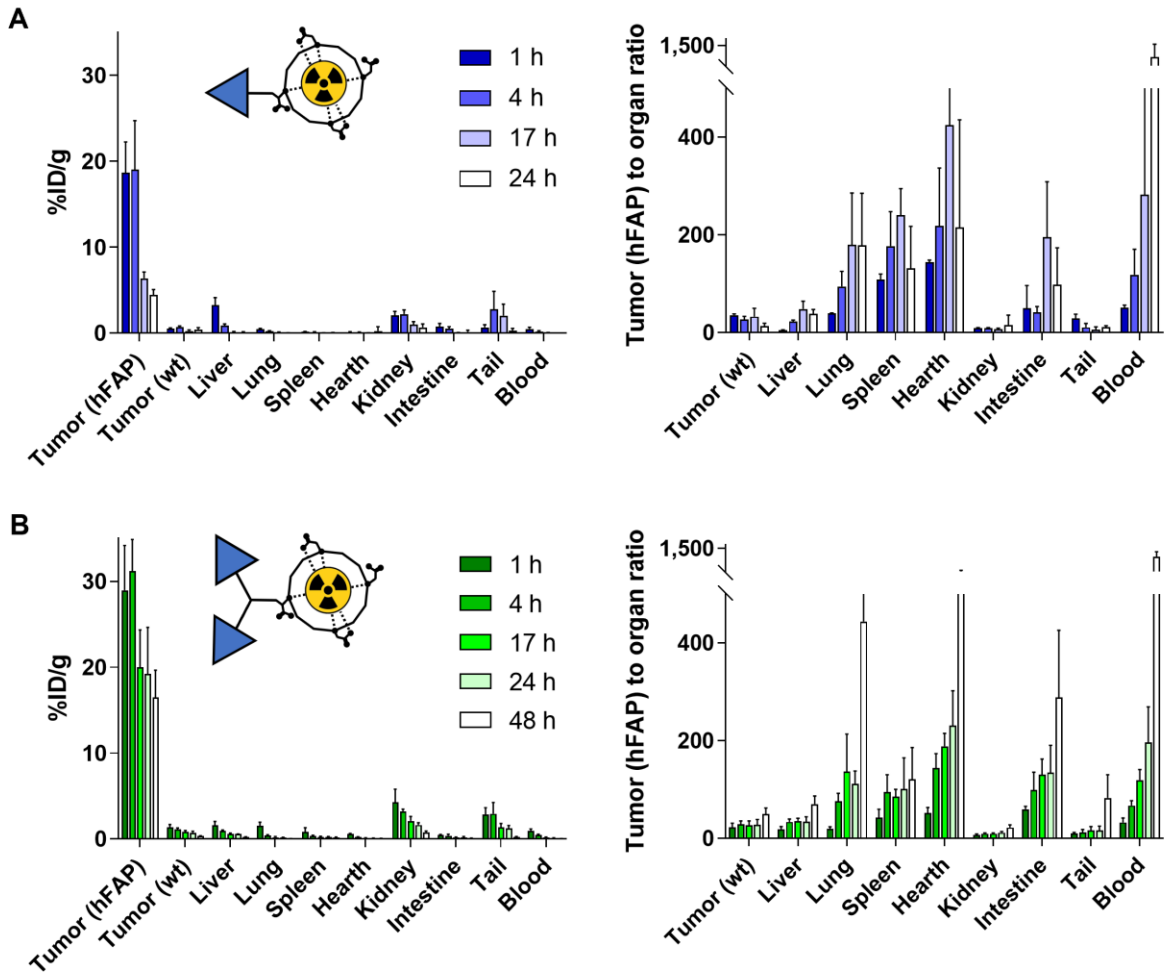

Figure 4. Quantitative *in vivo* biodistribution and tumour-to-organ ratio of (*A*) ^{177}Lu-OncoFAP (compound 3) and (*B*) ^{177}Lu-BiOncoFAP (compound 6) at different time points after intravenous administration (250 nmol/kg, 50 MBq/kg) in mice bearing HT-1080.wt and HT-1080.hFAP tumours.

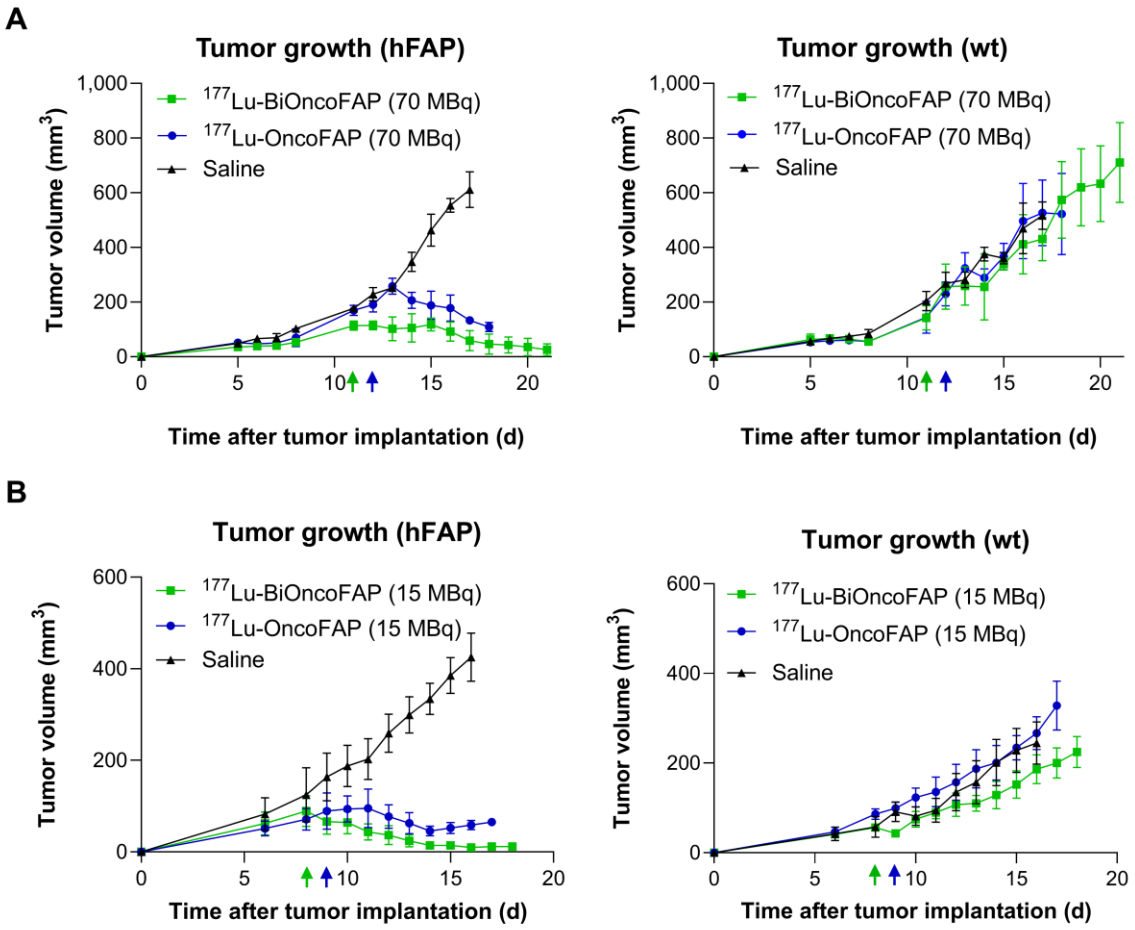

Figure 5. Therapeutic activity after a single administration (250 nmol/kg) of ^{177}Lu-OncoFAP (compound 3) and ^{177}Lu-BiOncoFAP (compound 6) in Balb/c nu/nu mice bearing HT-1080.hFAP tumour in the right flank and HT-1080.wt tumour in the left flank at a dose of (*A*) 70 MBq/mouse or (*B*) 15 MBq/mouse. The efficacy of the different treatments was assessed by daily measurement of tumour volume (mm^3) after administration of the different compounds. Data points represent mean tumour volume ± SEM.

References

1. Dal Corso A. Targeted small-molecule conjugates: the future is now. *ChemBioChem*. 2020;21:3321-3322.

2. Sun X, Li Y, Liu T, Li Z, Zhang X, Chen X. Peptide-based imaging agents for cancer detection. *Adv Drug Deliv Rev*. 2017;110-111:38-51.

3. Siva S, Udovicich C, Tran B, Zargar H, Murphy DG, Hofman MS. Expanding the role of small-molecule PSMA ligands beyond PET staging of prostate cancer. *Nat Rev Urol.* 2020;17:107-118.

4. Ballinger JR. Theranostic radiopharmaceuticals: Established agents in current use. *Br J Radiol*. 2018;91:20170969.

5. Turner JH. An introduction to the clinical practice of theranostics in oncology. *Br J Radiol*. 2018;91:20180440.

6. Lenzo NP, Meyrick D, Turner JH. Review of gallium-68 PSMA PET/CT imaging in the management of prostate cancer. *Diagnostics.* 2018;8:16.

7. Turner JH. Recent advances in theranostics and challenges for the future. *Br J Radiol*. 2018;91:20170893.

8. Herrero Álvarez N, Bauer D, Hernández-Gil J, Lewis JS. Recent advances in radiometals for combined imaging and therapy in cancer. *ChemMedChem*. 2021;16:2909-2941.

9. Hennrich U, Kopka K. Lutathera®: The first FDA- and EMA-approved radiopharmaceutical for peptide receptor radionuclide therapy. *Pharmaceuticals.* 2019;12:114.

10. Strosberg J, El-Haddad G, Wolin E, et al. Phase 3 trial of ^{177}Lu-DOTATATE for midgut neuroendocrine tumours . *N Engl J Med*. 2017;376:125-135.

11. Sartor O, de Bono J, Chi KN, et al. Lutetium-177–PSMA-617 for metastatic castration-resistant prostate cancer. *N Engl J Med*. 2021;385:1091-1103.

12. Calais J. FAP: the next billion dollar nuclear theranostics target? *J Nucl Med*. 2020;61:163-165.

13. Kratochwil C, Flechsig P, Lindner T, et al. ^{68}Ga-FAPI PET/CT: Tracer uptake in 28 different kinds of cancer. *J Nucl Med*. 2019;60:801-805.

14. Backhaus P, Burg M, Roll W, et al. A new horizon for breast cancer staging: first evidence from simultaneous PET-MRI targeting the fibroblast activating protein (FAP). *Nukl - Nucl*. 2021;60:L10.

15. Backhaus P, Burg MC, Roll W, et al. Simultaneous FAPI PET/MRI targeting the fibroblast-activation protein for breast cancer. *Radiology*. 2022;302:39-47.

16. Lo A, Wang LCS, Scholler J, et al. Tumour-promoting desmoplasia is disrupted by depleting FAP-expressing stromal cells. *Cancer Res*. 2015;75:2800-2810.

17. Mona CE, Benz MR, Hikmat F, et al. Correlation of ^{68}Ga-FAPi-46 PET biodistribution with FAP expression by immunohistochemistry in patients with solid cancers: a prospective translational exploratory study. *J Nucl Med*. 2021;63(5).

18. Millul J, Bassi G, Mock J, et al. An ultra-high-affinity small organic ligand of fibroblast activation protein for tumour-targeting applications. *Proc Natl Acad Sci*. 2021;118:e2101852118.

19. Backhaus P, Gierse F, Burg M C, et al. Translational imaging of the fibroblast activation protein (FAP) using the new ligand [^{68}Ga]Ga-OncoFAP-DOTAGA. *Eur J Nucl Med Mol Imaging.* 2021:1-11.

20. Mansi R, Fani M. Radiolabeled peptides for cancer imaging and therapy: from bench-to-

bedside. *Chimia (Aarau)*. 2021;75:500-504.

21. Zhao L, Niu B, Fang J, et al. Synthesis, preclinical evaluation, and a pilot clinical PET imaging study of ^{68}Ga-labeled FAPI dimer. *J Nucl Med*. 2021;63(5).

22. Jones W, Griffiths K, Barata PC, Paller CJ. PSMA Theranostics: review of the current status of PSMA-targeted imaging and radioligand therapy. *Cancers.* 2020;12:1367.

23. Schäfer M, Bauder-Wüst U, Leotta K, et al. A dimerized urea-based inhibitor of the prostatespecific membrane antigen for ^{68}Ga-PET imaging of prostate cancer. *EJNMMI Res*. 2012;2:1-11.

24. Gupta SK, Singla S, Thakral P, Bal CS. Dosimetric analyses of kidneys, liver, spleen, pituitary gland, and neuroendocrine tumours of patients treated with ^{177}Lu-DOTATATE. *Clin Nucl Med*. 2013;38:188-194.

25. Schuchardt C, Zhang J, Kulkarni HR, Chen X, Mueller D, Baum RP. Prostate-specific membrane antigen radioligand therapy using ^{177}Lu-PSMA and ^{177}Lu-PSMA-617 in patients with metastatic castration-resistant prostate cancer: comparison of safety, biodistribution and dosimetry. *J Nucl Med*. 2021;63(5).

26. Kaghazchi F, Aghdam RA, Haghighi S, Vali R, Adinehpour Z. ^{177}Lu-FAPI therapy in a patient with end-stage metastatic pancreatic adenocarcinoma. *Clin Nucl Med*. 2022;47:243-245.

27. Meyer C, Dahlbom M, Lindner T, et al. Radiation dosimetry and biodistribution of ^{68}Ga-FAPI-46 PET imaging in cancer patients. *J Nucl Med*. 2020;61:1171-1177.

28. Loktev A, Lindner T, Burger EM, et al. Development of fibroblast activation protein–targeted radiotracers with improved tumour retention. *J Nucl Med*. 2019;60:1421-1429.

29. Li H, Ye S, Li L, Zhong J, Yan Q, Zhong Y, Feng P, Hu K. ^{18}F- or ^{177}Lu-labeled bivalent

ligand of fbroblast activation protein with high tumor uptake and retention. *Eur J Nucl Med Mol Imaging*. 2022:1-11.

30. Tarli L, Balza E, Viti F, et al. A high-affinity human antibody that targets tumoural blood vessels. *Blood*. 1999;94:192-198.

31. Tönnesmann R, Meyer PT, Eder M, Baranski AC. [^{177}Lu]Lu-PSMA-617 salivary gland uptake characterized by quantitative in vitro autoradiography. *Pharmaceuticals.* 2019;12:18.

32. Geenen L, Nonnekens J, Konijnenberg M, Baatout S, De Jong M, Aerts A. Overcoming nephrotoxicity in peptide receptor radionuclide therapy using [^{177}Lu]Lu-DOTA-TATE for the treatment of neuroendocrine tumours. *Nucl Med Biol*. 2021;102-103:1-11.

33. Navalkissoor S, Grossman A. Targeted alpha particle therapy for neuroendocrine tumours: the next generation of peptide receptor radionuclide therapy. *Neuroendocrinology*. 2019;108:256-264.

34. Frey K, Neri D. Antibody-based targeting of tumour vasculature and stroma. *Tumour-Associated Fibroblasts and their Matrix*. 2011:419-450.

35. Liu Y, Watabe T, Kaneda-Nakashima K, et al. Fibroblast activation protein targeted therapy using [^{177}Lu]FAPI-46 compared with [^{225}Ac]FAPI-46 in a pancreatic cancer model. *Eur J Nucl Med Mol Imaging.* 2021;49:871-880.

36. Gaertner FC, Kessler H, Wester HJ, Schwaiger M, Beer AJ. Radiolabelled RGD peptides for imaging and therapy. *Eur J Nucl Med Mol Imaging*. 2012;39:126-138.

37. Liu S. Radiolabeled cyclic RGD peptides as integrin αvβ3-targeted radiotracers: maximizing binding affinity via bivalency. *Bioconjug Chem*. 2009;20:2199-2213.

38. Krall N, Pretto F, Neri D. A bivalent small molecule-drug conjugate directed against

carbonic anhydrase IX can elicit complete tumour regression in mice. *Chem Sci*. 2014;5:3640-3644.

39. Liu S. Radiolabeled multimeric cyclic RGD peptides as integrin αvβ3 targeted radiotracers for tumour imaging. *Mol Pharm*. 2006;3:472-487.

40. Chittasupho C. Multivalent ligand: design principle for targeted therapeutic delivery approach. *Ther Deliv*. 2012;3:1171-1187.

41. Ballal S, Yadav MP, Moon ES, et al. First-in-human results on the biodistribution, pharmacokinetics, and dosimetry of [^{177}Lu]Lu-DOTA.SA.FAPi and [^{177}Lu]Lu-DOTAGA.(SA.FAPi)2. *Pharmaceuticals.* 2021;14:1212.

42. Qin C, Song Y, Cai W, Lan X. Dimeric FAPI with potential for tumour theranostics. *Am J Nucl Med Mol Imaging*. 2021;11:537.

43. Baum RP, Schuchardt C, Singh A, et al. Feasibility, biodistribution and preliminary dosimetry in peptide-targeted radionuclide therapy (PTRT) of diverse adenocarcinomas using ^{177}Lu-FAP-2286: first-in-human results. *J Nucl Med*. 2021;63(5).

44. Zhao L, Shang Q, Wu H, Lin Q. Fibroblast activation protein-based theranostics in cancer research: a state-of-the-art review. *Theranostics.* 2022; 12(4):1557-1569.

45. Nishio M, Okamoto I, Murakami H, et al. Preclinical evaluation of FAP-2286, a peptide-targeted radionuclide therapy (PTRT) to fibroblast activation protein alpha (FAP). *Ann Oncol*. 2020;31:S488.

46. Assadi M, Rekabpour SJ, Jafari E, et al. Feasibility and therapeutic potential of ^{177}Lu-fibroblast activation protein inhibitor-46 for patients with relapsed or refractory cancers: a preliminary study. *Clin Nucl Med*. 2021;46:523-530.

Graphical Abstract

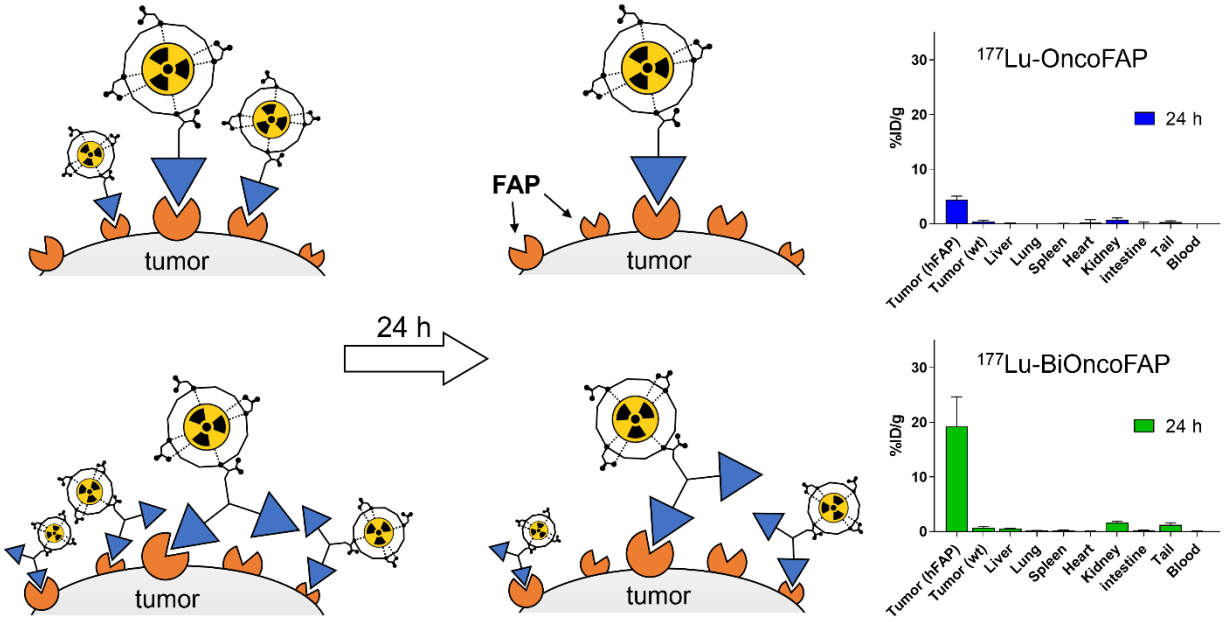

Supplementary Information

A novel dimeric FAP-targeting small molecule-radio conjugate with high and prolonged tumour uptake

Andrea Galbiati[1,*], Aureliano Zana[1,*], Matilde Bocci[1], Jacopo Millul[1], Abdullah Elsayed[1], Jacqueline Mock[1], Dario Neri[2,3†], Samuele Cazzamalli[1†]

[1] Philochem AG, R&D department, CH-8112 Otelfingen, Switzerland;

[2] Swiss Federal Institute of Technology, Department of Chemistry and Applied Biosciences, CH-8093 Zurich, Switzerland;

[3] Philogen S.p.A., 53100 Siena, Italy.

* First authors, contributed equally to this work

† Corresponding authors:

Dr. Samuele Cazzamalli - samuele.cazzamalli@philochem.ch

Prof. Dario Neri - neri@pharma.ethz.ch

Index

CHEMISTRY

Materials and Methods

Liquid Chromatography-Mass Spectrometry (LC-MS) spectra presented were recorded on an Agilent 6100 Series Single Quadrupole MS system combined with an Agilent 1200 Series LC, using an InfinityLab Poroshell 120 EC-C18 Column, 2.7 µm, 4.6 × 50 mm at a flow rate of 0.8 mL/min, 10% ACN in 0.1% aq. HCOOH to 100% ACN in 3 or 10 min.

Reversed-phase high-pressure liquid chromatography (RP-HPLC) were performed on an Agilent 1200 Series RP-HPLC with PDA UV detector, using a Synergi 10µm, MAX-RP 80Å 10 × 250 mm C18 column at a flow rate of 5 mL/min with linear gradients of solvents A and B (A = Millipore water with 0.1% TFA, B = ACN with 0.1% TFA).

High-Resolution mass spectrometry (HR-MS) were performed on a Q Exactive Mass Spectrometer (Thermo Fisher Scientific). The analyte was injected directly into the MS at a flow rate of 4 µL/min. Both MS1 and MS2 spectra were recorded. MS1 spectra were obtained with a resolution of 70000. MS2 spectra were obtained by inducing fragmentation of the molecule with a NCE (normalized collision energy) =25 and with a resolution of 70000.

Synthetic Schemes

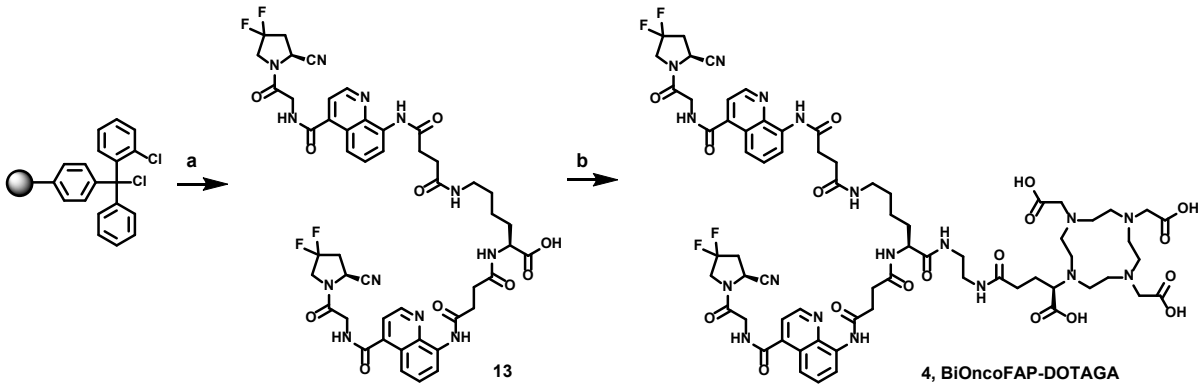

Supplemental Scheme 1. Synthesis of BiOncoFAP-DOTAGA (**4**). Reagents and conditions: a) i) NHFmoc-L-Lys(Fmoc)-OH, NMM, dry DCM, 6h, r.t.; ii) MeOH, NMM, dry DCM, 30 min, r.t.; iii) Piperidine/DMF 20% v/v, 20 min, r.t.; iv) OncoFAP-COOH, HATU, DIPEA; DMF, 1h, r.t.; v) TFA/DCM 30% v/v, 1h, r.t.; b) i) *N*-hydroxysuccinimide, HATU, DIPEA, DMF, 30 min, r.t.; ii) (R)-DOTA-GA-NH_2, overnight, r.t.

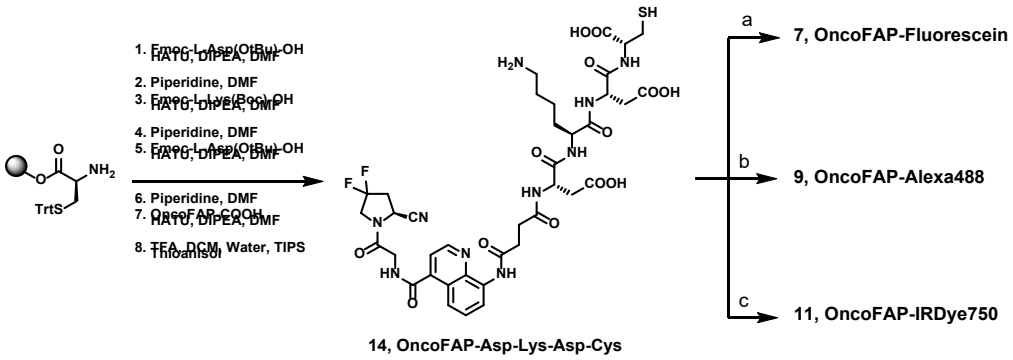

Supplemental Scheme 2. Synthesis of OncoFAP-Fluorescein (**7**), OncoFAP-Alexa488 (**9**) and OncoFAP-IRDye750 (**11**). Reagents and conditions: a) Maleimido-Fluorescein, DMF, PBS, 3 h, r.t.; b) AlexaFluor488-C5-Maleimide, DMSO, PBS, 3 h, r.t.; c) IRDye750-Maleimide, DMF, PBS, 3h, r.t.

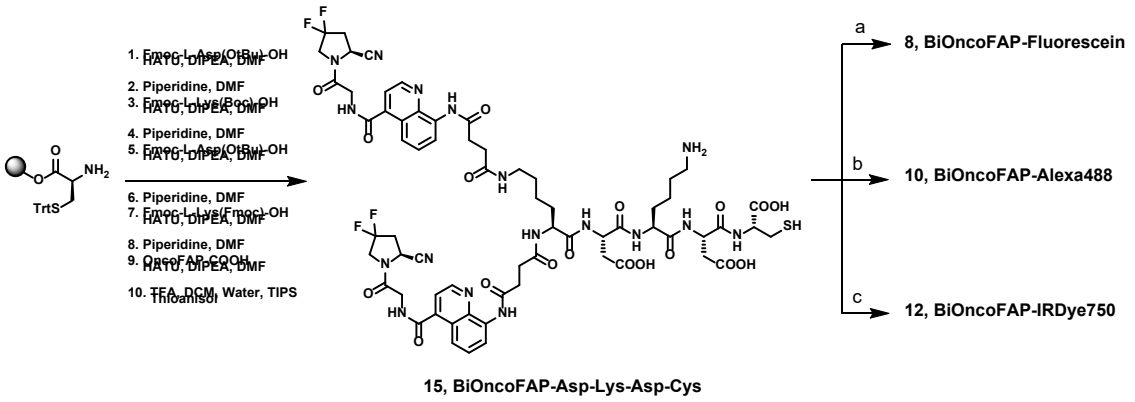

Supplemental Scheme 3. Synthesis of BiOncoFAP-Fluorescein (**8**), BiOncoFAP-Alexa488 (**10**) and BiOncoFAP-IRDye750 (**12**). Reagents and conditions: a) Maleimido-Fluo, DMF, PBS, 3 h, r.t.; b) AlexaFluor488-C5-Maleimide, DMSO, PBS, 3 h, r.t.; c) IRDye750-Maleimide, DMF, PBS, 3h, r.t.

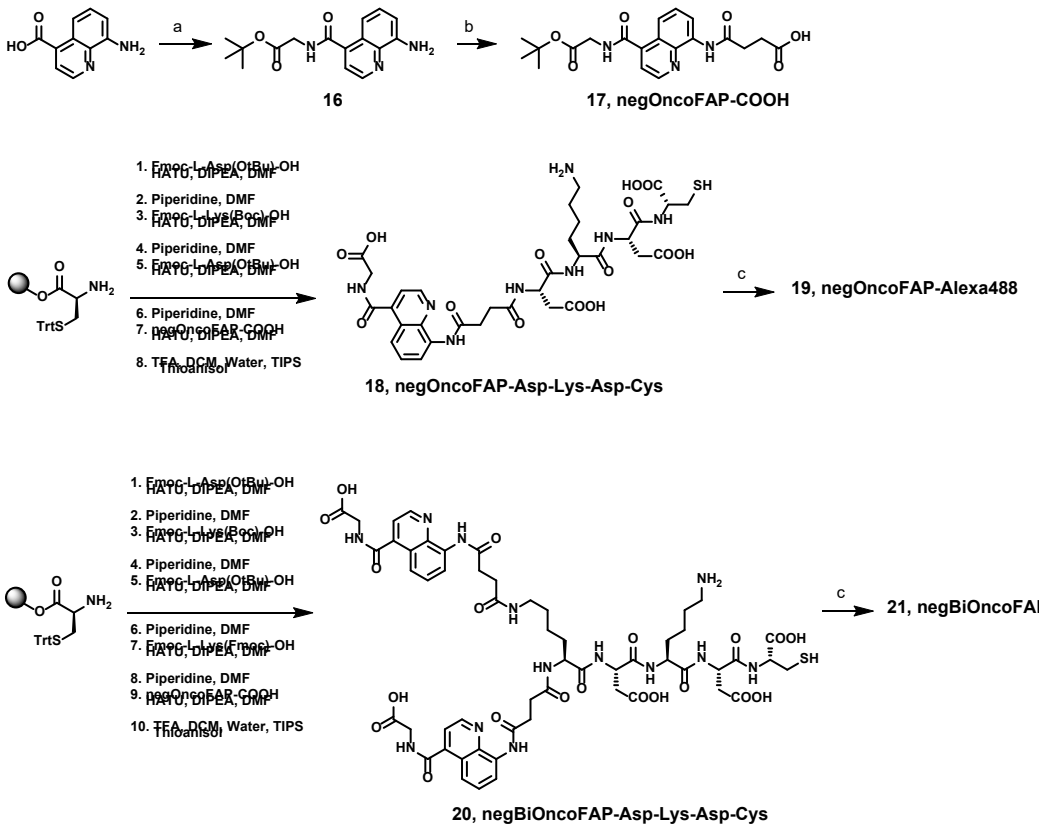

Supplemental Scheme 4. Synthesis of negOncoFAP-Alexa488 (**19**) and negBiOncoFAP-Alexa488 (**21**). Reagents and conditions: a) Gly-OtBu*HCl, HATU, DIPEA, DCM/DMF, 30 min, 0°C to r.t.; b) Succinic anhydride, DMAP, THF, 1 h, 55°C; c) AlexaFluor488-C5-Maleimide, DMSO, PBS, 3 h, r.t.

Synthesis of BiOncoFAP-COOH (13)

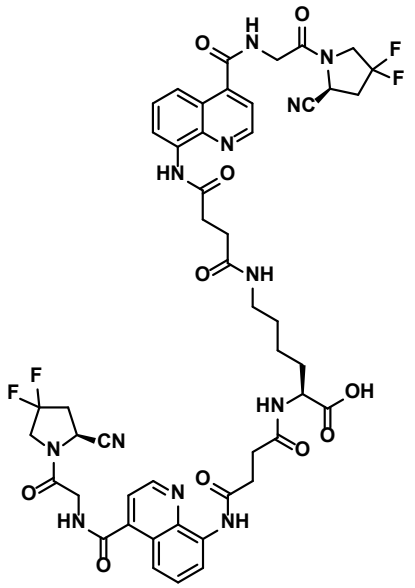

To a solid-phase synthesis syringe, 2-chlorotrityl resin (300 mg) was added and then swollen with dry DCM for 15 min. Fmoc-L-Lys(Fmoc)-OH (89 mg, 0.15 mmol, 1 eq.) and 4-Methylmorpholine (45 µL, 0.40 mmol, 2.7 eq.) were sequentially added to the resin and the mixture was allowed to react for 3 h. Next, a capping step with methanol / 4-Methylmorpholine / DCM (1:2:7 ratio, 5 mL, 30 min) was carried out, following by a wash with DMF and Fmoc-removal with 20% solution of Piperidine in DMF (10 mL). The resin was then treated with a solution of OncoFAP-COOH (137 mg, 0.300 mmol, 2.0 eq.), HATU (86 mg, 0.22 mmol, 1.5 eq.) and DIPEA (97 µL, 0.75 mmol, 5.0 eq.) in DMF (5 mL) for 1 h. After multiple washing with DMF, the resin was submitted to the cleavage with 30% solution of TFA in DCM (10 mL) for 1 h. The cleaved solution was recovered, concentrated under *vacuo* and purified by Reverse Phase Flash-Chromatography (gradient: water/acetonitrile + 0.1% FA 98:2 to 0:100 in 45 min). The fractions were collected and lyophilized to afford a white solid (30 mg, 0.029 mmol, 19% yield). MS(ES+) m/z 1029.3 $(M+H)^+$

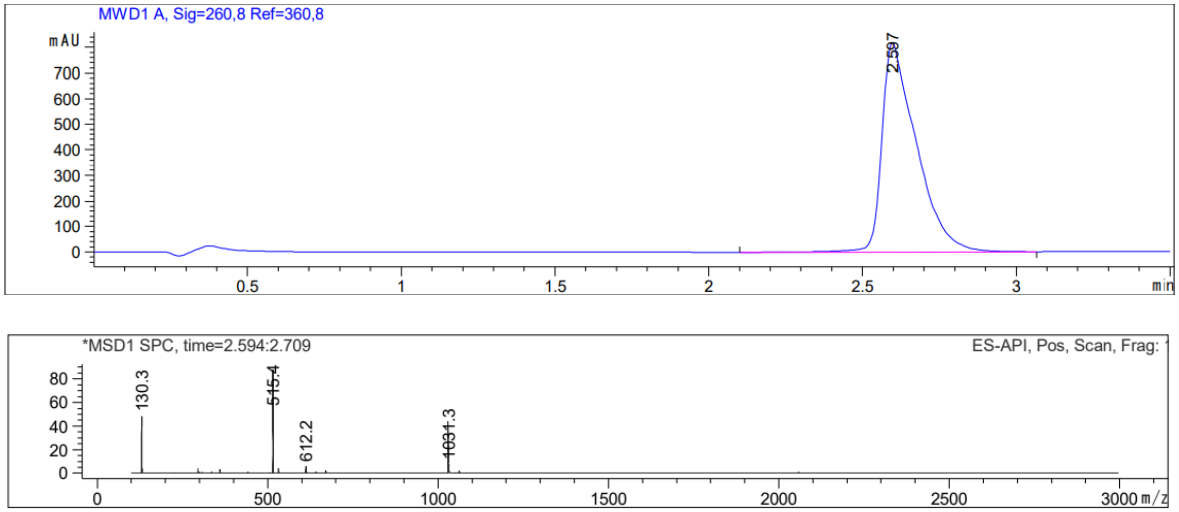

Synthesis of BiOncoFAP-DOTAGA (4)

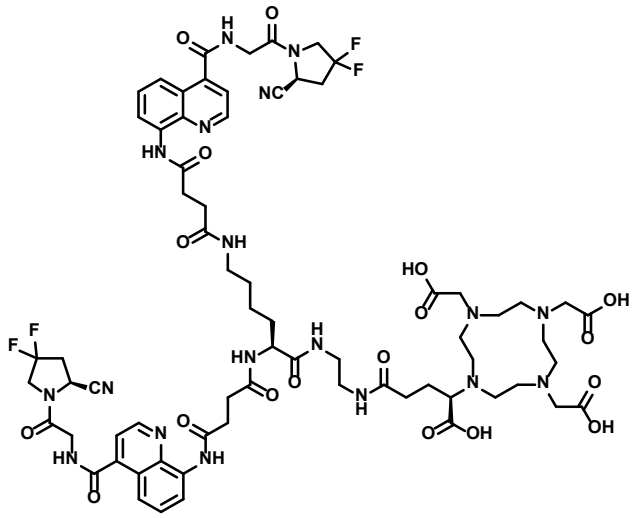

N-Hydroxysuccinimide (40 mg, 0.35 mmol, 2 eq.), HATU (80 mg, 0.21 mmol, 1.2 eq.) and DIPEA (0.15 mL, 0.88 mmol, 5 eq.) were added to a solution of BiOncoFAP-COOH (180 mg, 0.175 mmol, 1 eq.) in dry DMF (5 mL). The reaction solution was stirred for 30 minutes at room temperature, then (*R*)-DOTA-GA-NH_2 (180 mg, 0.35 mmol, 2 eq.) was added. The resulting mixture was stirred vigorously overnight, then diluted with milliQ water (5 mL) and purified via RP-HPLC (90:10 to 0:100 ACN/water + 0.1% TFA in 12 min). The desired fractions were collected and lyophilized to afford a white solid. (140 mg, 52%).

HPLC-UV:

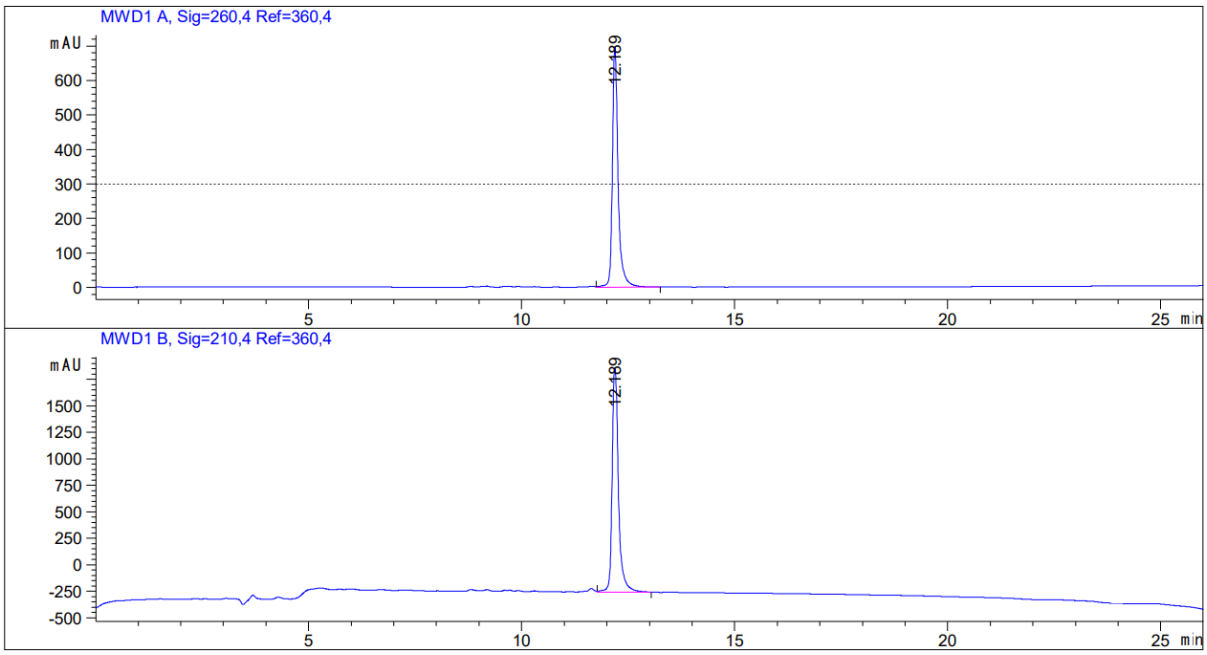

LC-UV/MS:

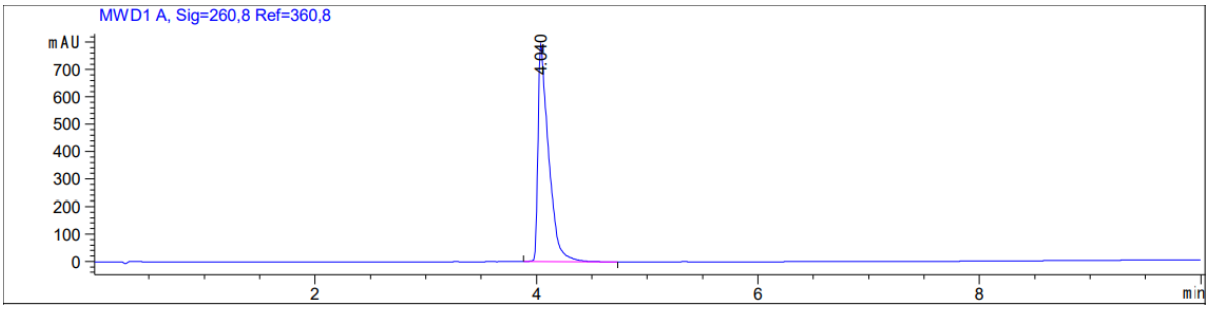

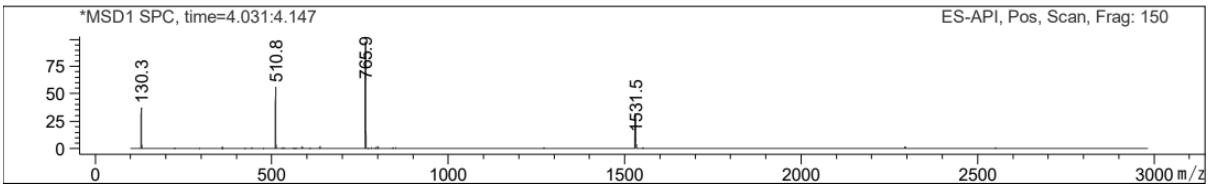

HR-MS. Predicted M/z = 1529.62198; Experimental M/z = 1529.6222; Accuracy = 0.14 ppm

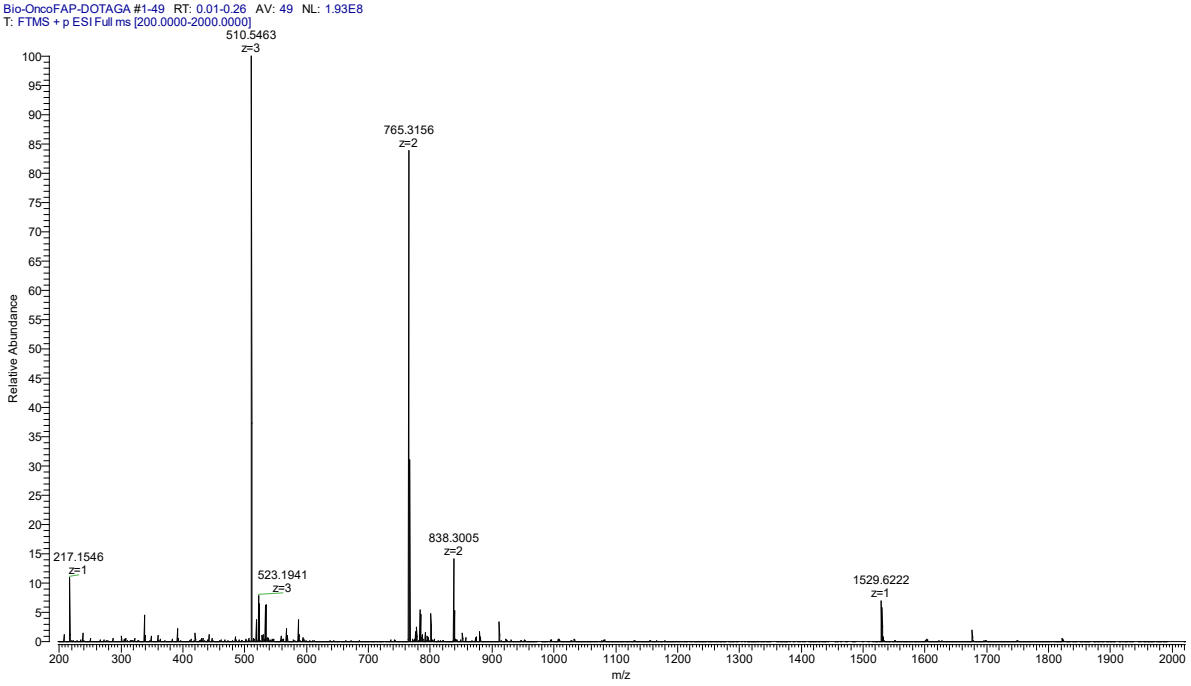

Synthesis of ^{nat}Lu-OncoFAP-DOTAGA (2)

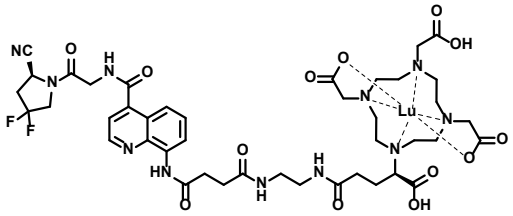

To a solution of OncoFAP-DOTAGA (compound **1**, 0.96 mg, 1 µmol, 1 eq.) in 300 µL acetate buffer (aqueous solution, 1 M, pH 8), a freshly prepared solution of $LuCl_3$ hexahydrate (0.78 mg, 2 µmol, 2 eq.) in 0.05N HCl (1.5 mL) was added. The resulting mixture was stirred at 95°C for 10-15 minutes, then purified via RP-HPLC (90:10 to 0:100 ACN/water + 0.1% TFA in 12 min). The desired fractions were collected and lyophilized to afford a white solid. (0.8 mg, 71%)

LC-MS:

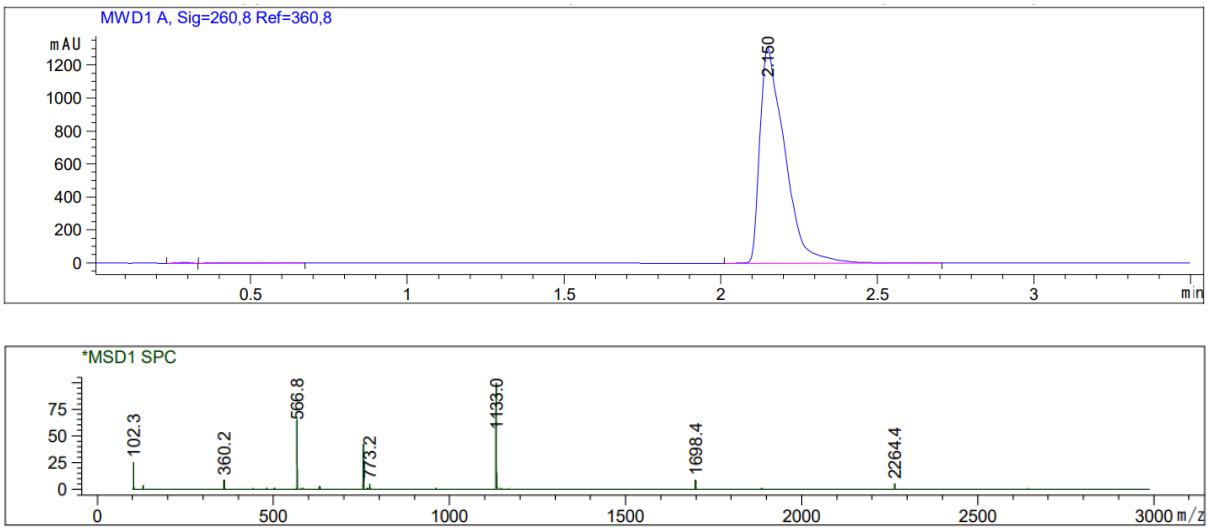

HR-MS: Predicted M/z = 1132.31946; Experimental M/z = 1132.32056; Accuracy = 0.97 ppm

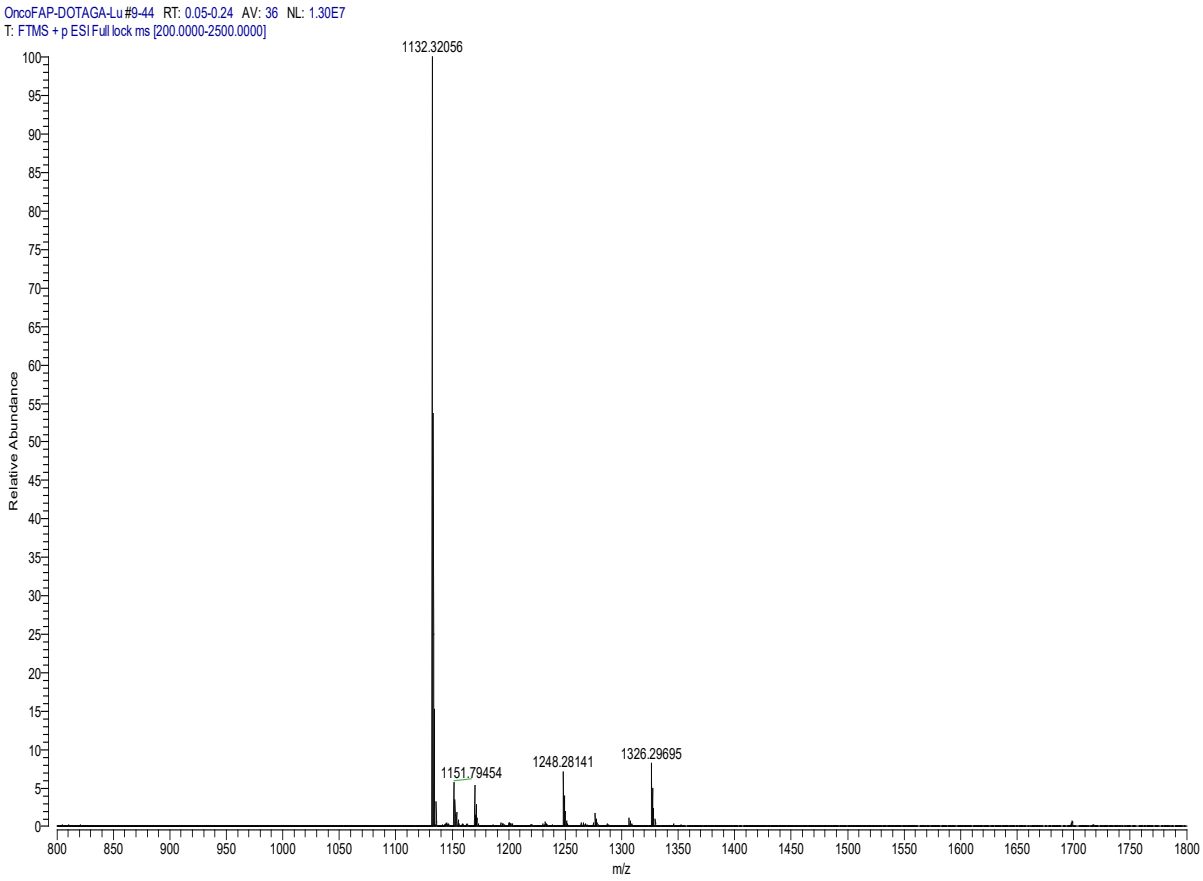

Synthesis of ^{nat}Lu-BiOncoFAP-DOTAGA (5)

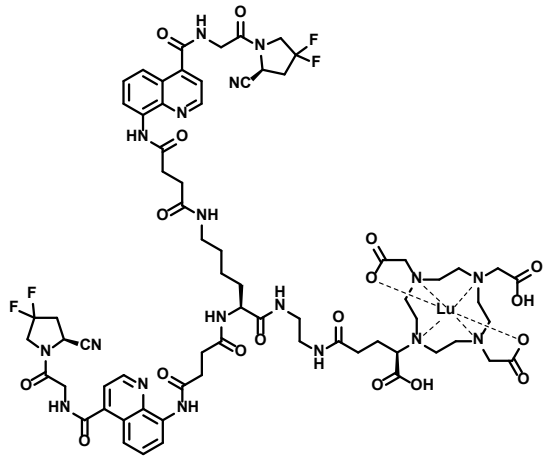

To a solution of BiOncoFAP-DOTAGA (compound **4**, 1.5 mg, 1 µmol, 1 eq.) in 300 µL acetate buffer (aqueous solution, 1 M, pH 8), a freshly prepared solution of $LuCl_3$ hexahydrate (0.78 mg, 2 µmol, 2 eq.) in 0.05N HCl (1.5 mL) was added. The resulting mixture was stirred at 95°C for 10-15 minutes, then purified via RP-HPLC (90:10 to 0:100 ACN/water + 0.1% TFA in 12 min). The desired fractions were collected and lyophilized to afford a white solid. (1.2 mg, 67%)

LC-MS:

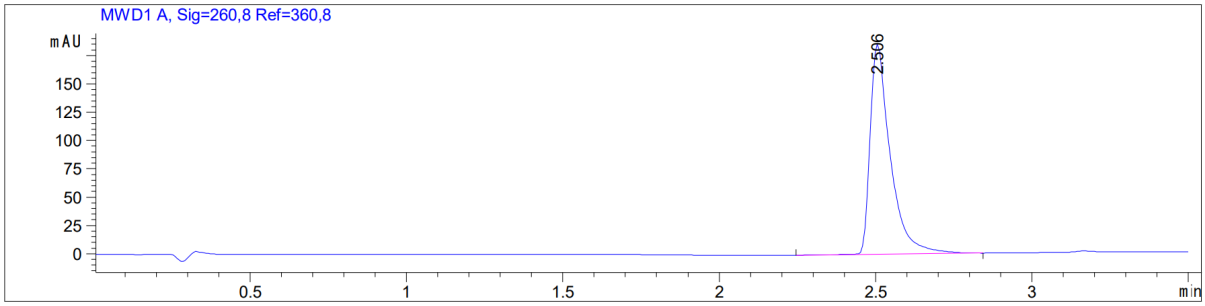

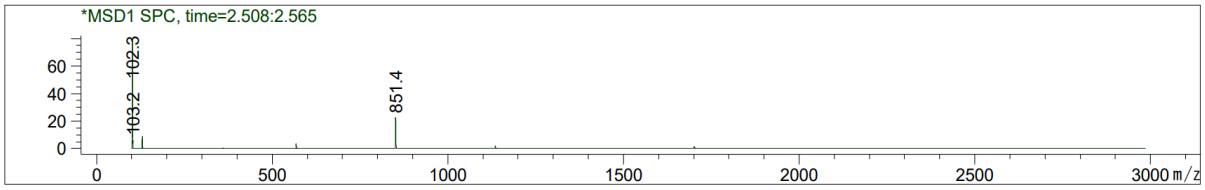

HRMS: Predicted M/z = 1702.54711; Experimental M/z = 1702.54660; Accuracy = 0.30 ppm

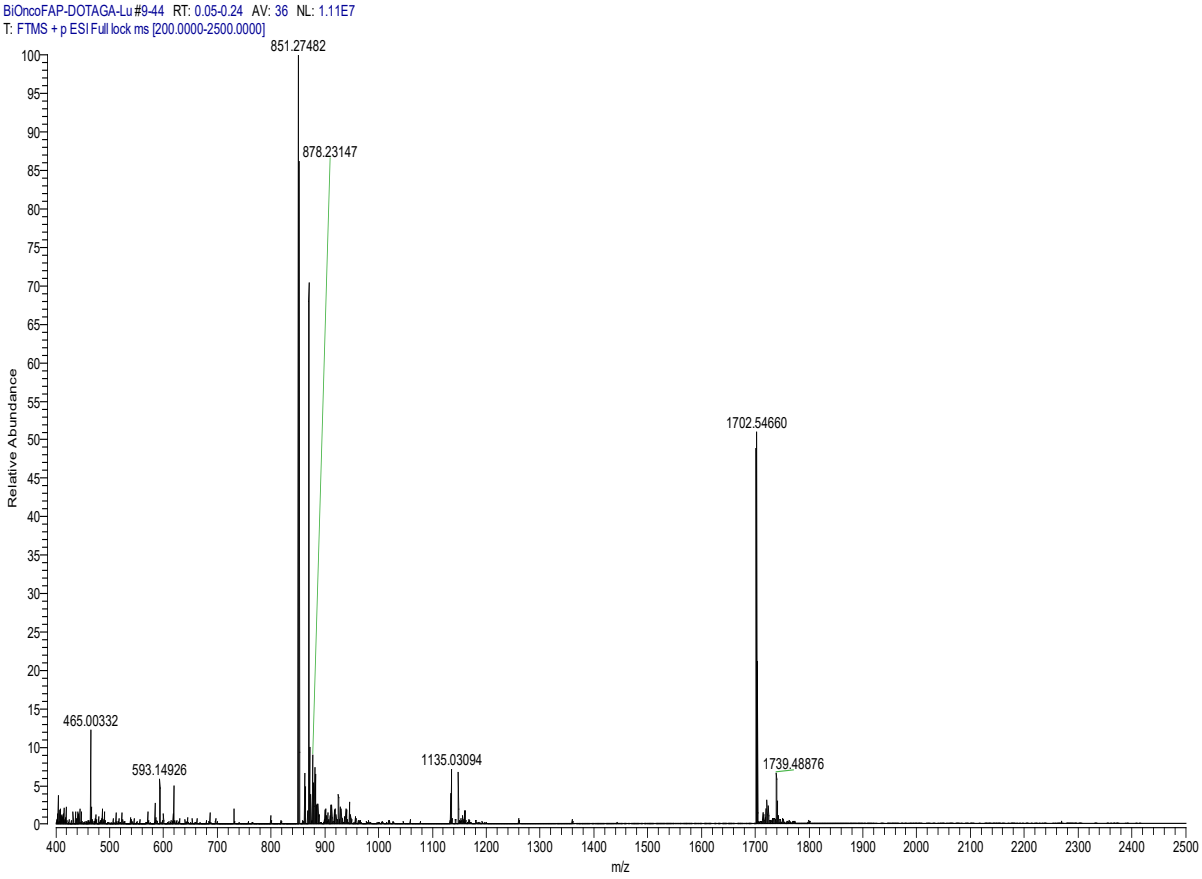

Synthesis of BiOncoFAP-Asp-Lys-Asp-Cys (15)

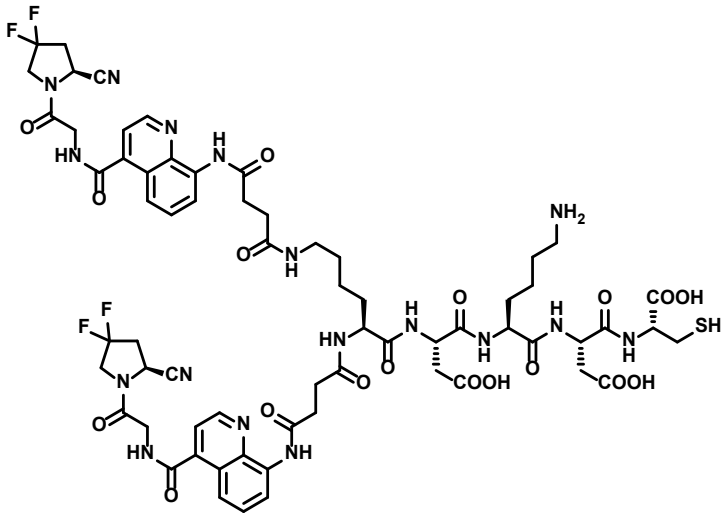

To a solid-phase synthesis syringe, H-Cys(Trt)-2-CT-polystyrene resin (900 mg) was added and then swollen with DMF for 15 min. Fmoc-L-Asp(OtBu)-OH (444 mg, 1.08 mmol, 2 eq.), HATU (411 mg, 1.08 mmol, 2 eq.) and DIPEA (377 µL, 2.16 mmol, 4 eq.) were sequentially added to the resin. The mixture was allowed to react for 2 h, then treated with a 20% solution of Piperidine in DMF (10 mL) for the Fmoc-removal and washed several times with DMF. The resin was then treated with a solution of Fmoc-L-Lys(Boc)-OH (506 mg, 1.08 mmol, 2 eq.), HATU (411 mg, 1.08 mmol, 2 eq.) and DIPEA (377 µL, 2.16 mmol, 4 eq.) in DMF (10 mL) for 2 h, following Fmoc-removal with a 20% solution of Piperidine in DMF (10 mL). After washing with DMF, a solution of Fmoc-L-Asp(OtBu)-OH (444 mg, 1.08 mmol, 2 eq.), HATU (411 mg, 1.08 mmol, 2 eq.) and DIPEA (377 µL, 2.16 mmol, 4 eq.) in DMF (10 mL) was added to the resin. After 1 h, the resin was washed and treated with a 20% solution of Piperidine in DMF (10 mL). Subsequently, Fmoc-L-Lys(Fmoc)-OH (647 mg, 1.08 mmol, 2 eq.), HATU (411 mg, 1.08 mmol, 2 eq.) and DIPEA (377 µL, 2.16 mmol, 4 eq.) and DMF (10 mL) were added to the resin and the mixture was allowed to react for 2 h, following Fmoc-removal with 20% solution of Piperidine in DMF (10 mL). Lastly, the resin was treated with a solution of OncoFAP-COOH (992 mg, 2.16 mmol, 4 eq.), HATU (822 mg, 2.16 mmol, 4 eq.) and DIPEA (754 µL, 4.32 mmol, 8 eq.) in DMF (15 mL) for 2 h. The peptide was then cleaved from the resin using 15 mL of a solution of TFA/Triisopropylsilane/Thioanisol/water in DCM (30 : 5 : 2.5 : 2.5 : 60) for 1 h. The residue was concentrated under *vacuum*, resuspended in cold diethyl ether and centrifugated. The supernatant was discarded, and the pellet was dissolved in DMF and purified via RP-HPLC using a gradient of Water/ACN + 0.1% TFA in 7 min. The desired fractions were collected and lyophilized to afford a white solid. (136 mg, 17%)

MS(ES+) m/z 1490.5 $(M+H)^+$

Synthesis of BiOncoFAP-Fluorescein (8)

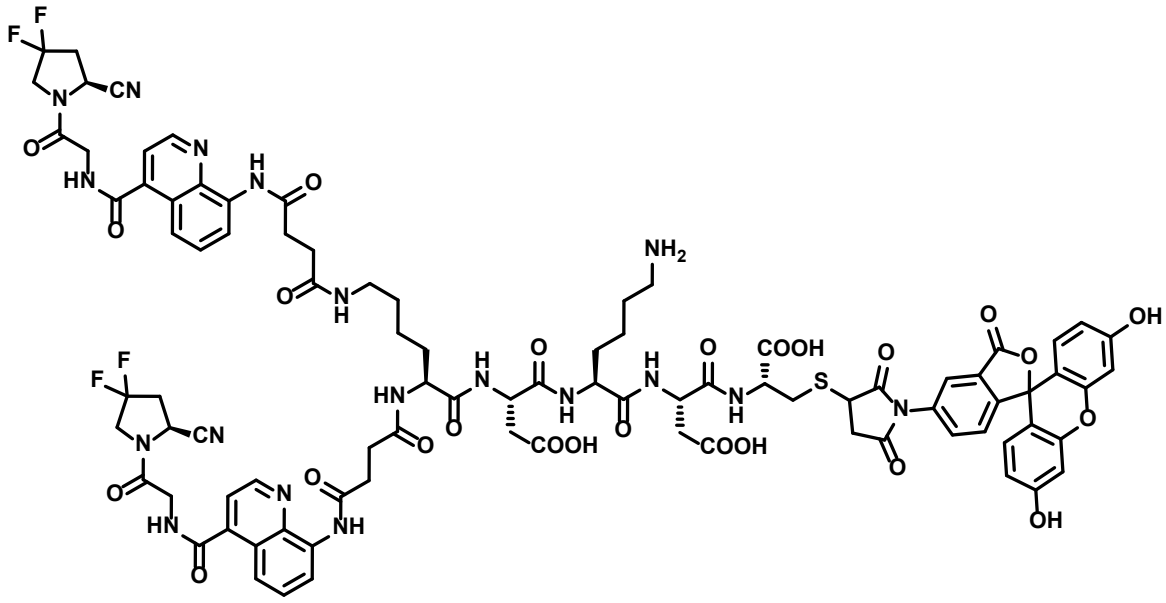

BiOncoFAP-Asp-Lys-Asp-Cys (1.00 mg, 0.59 µmol, 1.0 eq) is dissolved in PBS pH 7.4 (840 µL). Maleimido-Fluorescein (0.76 mg, 1.77 µmol, 3.0 eq) is added as dry DMF solution (160 µL). The reaction is stirred for 3 h. The crude material is purified by RP-HPLC (Water 0.1% TFA/ACN 0.1%TFA 95:5 to 2:8 in 20 min) and lyophilized, to obtain a yellow solid. (1.0 mg, 88%)

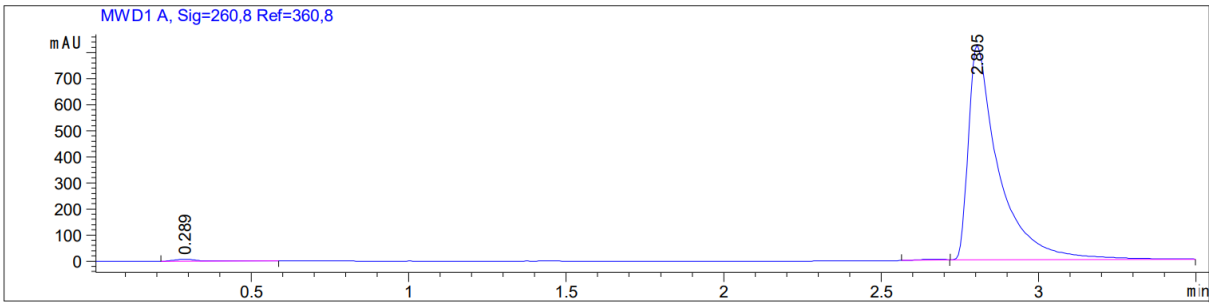

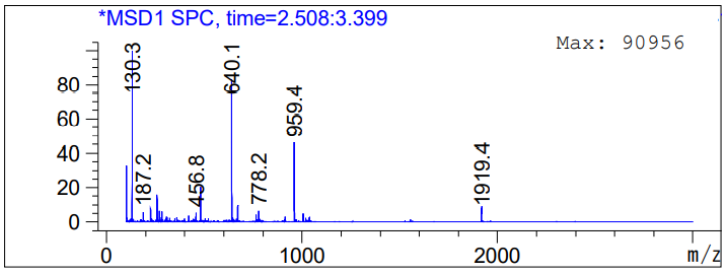

Synthesis of BiOncoFAP-Alexa488 (10)

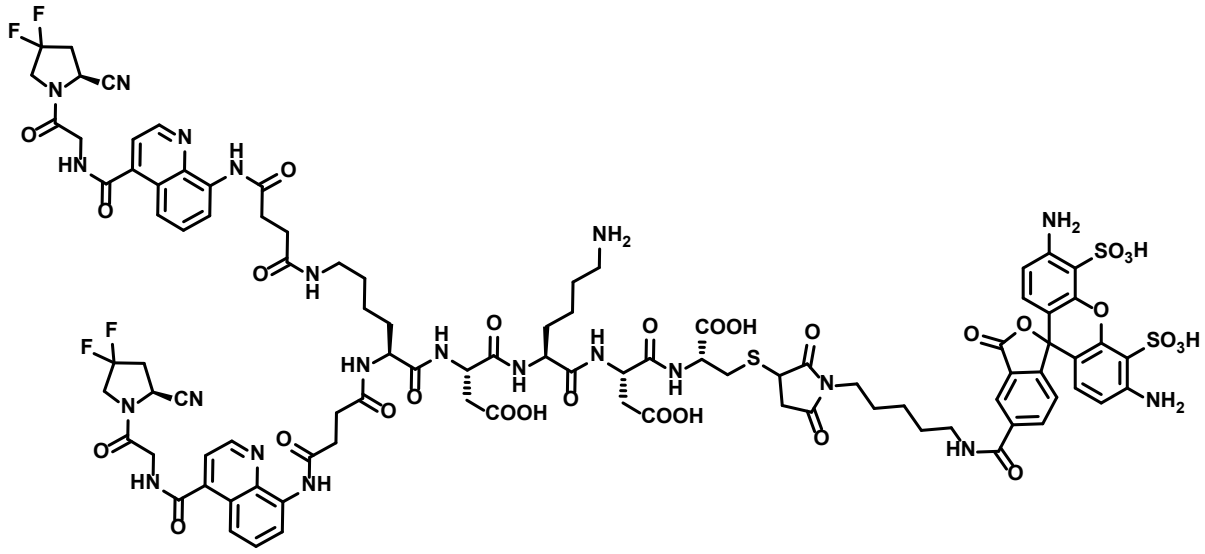

BiOncoFAP-Asp-Lys-Asp-Cys (1.0 mg, 0.59 µmol, 1.0 eq) is dissolved in PBS pH 7.4 (300 µL). Alexa FluorTM 15 488 C5 Maleimide (200 µg, 0.29 µmol, 0.5 eq) is added as dry DMSO solution (200 µL). The reaction is stirred for 3 h. The crude material is purified by RP-HPLC (Water 0.1% TFA/ACN 0.1%TFA 95:5 to 2:8 in 20 min) and lyophilized, to obtain an orange solid. (1.1 mg, 88%)

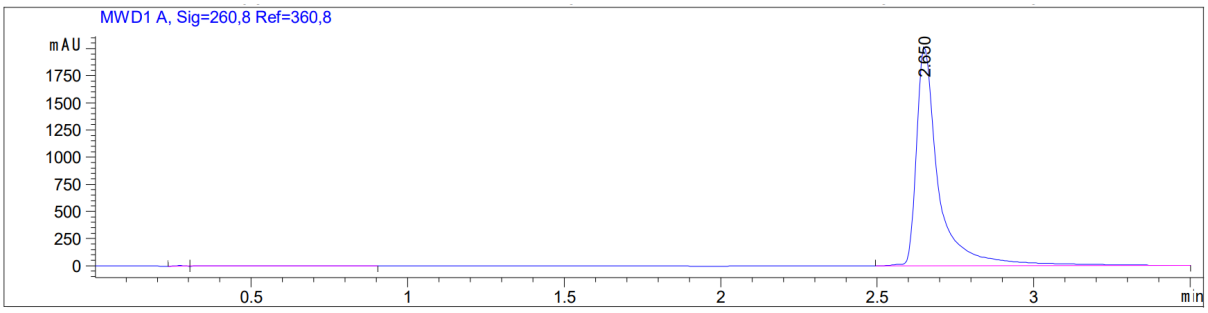

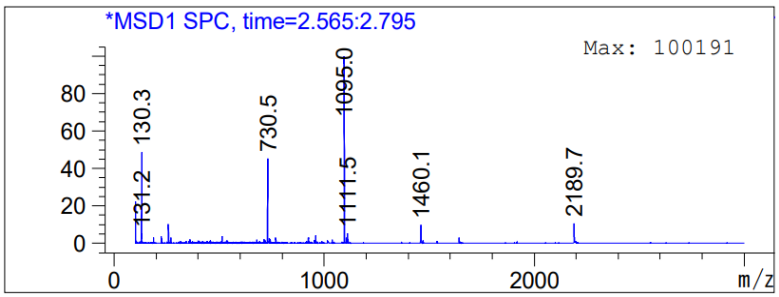

Synthesis of BiOncoFAP-IRDye750 (12)

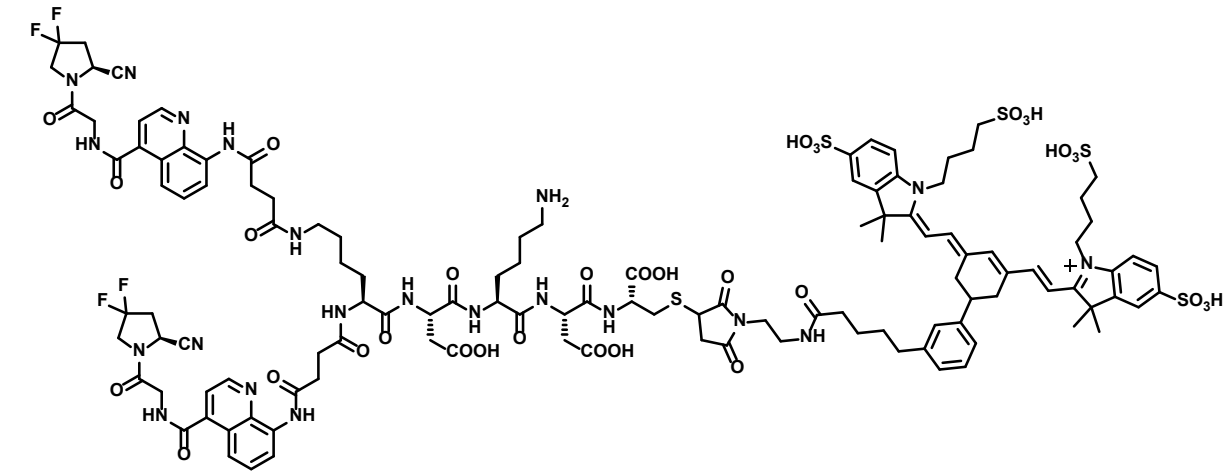

To a solution of BiOncoFAP-Asp-Lys-Asp-Cys (204 µg, 0.14 µmol, 1 eq.) in PBS pH=7.4 (200 µL) was added a solution of IRDye750 maleimide (150 µg, 0.12 µmol, 0.9 eq.) in DMSO (150 µL). The mixture was stirred at room temperature for 3 h and purified via RP-HPLC using a gradient of 90:10 to 50:50 water/ACN + 0.1% TFA in 7 min). The desired fractions were collected and lyophilized to afford a blue solid collect the desired fractions and lyophilize to afford a green solid. (0.2 mg, 54%)

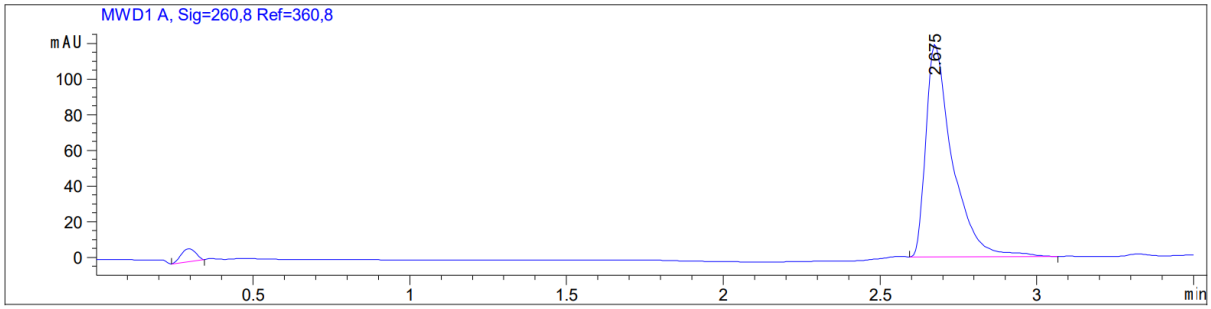

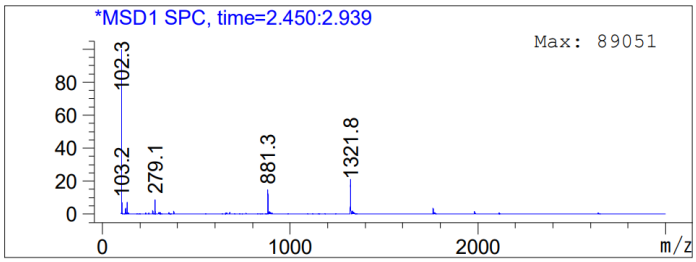

Synthesis of tert-butyl (8-aminoquinoline-4-carbonyl)glycinate (16)

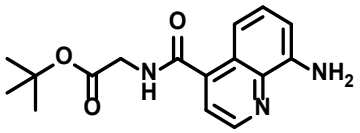

8-aminoquinoline-4-carboxylic acid (200 mg, 1.06 mmol, 1 eq.), HATU (401 mg, 1.06 mmol, 1 eq.) and Gly-OtBu*HCl (214 mg, 1.28 mmol, 1.2 eq.) were suspended in a 4:1 mixture of DCM/DMF (4 mL) and cooled to 0°C. DIPEA (0.74 mL, 4.25 mmol, 4 eq.) was added dropwise to the reaction mixture and stirred at room temperature for 30 min. The solution was transferred to a separatory funnel, diluted with DCM and washed with a saturated aqueous solution of $NaHCO_3$ and brine. The organic phase was dried over anhydrous Na_2SO_4, filtered and evaporated under reduced pressure to afford a brown oil. The crude was purified via flash column chromatography (100% DCM to 9:1 DCM/MeOH) to afford a yellow foam. (259 mg, 79%).

MS (ESI+), m/z 302.2

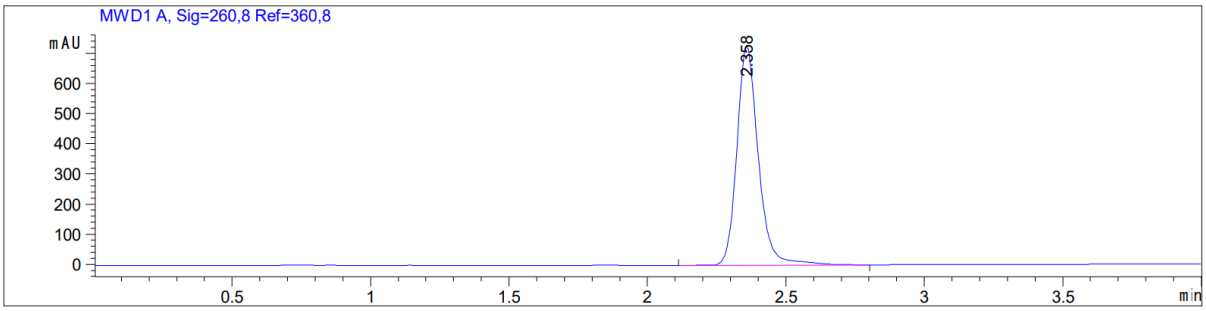

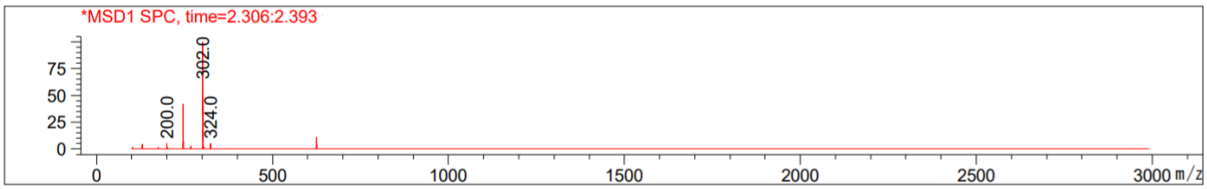

Synthesis of negOncoFAP-COOH (17)

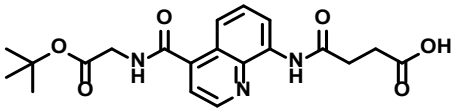

Compound **16** (259 mg, 0.86 mmol, 1 eq.), succinic anhydride (258 mg, 2.58 mmol, 3 eq.) and DMAP (52 mg, 0.43 mmol, 0.5 eq.) were dissolved in dry THF (5 mL). The mixture was heated at 55°C for 1h then cooled to room temperature, diluted with EtOAc and transferred to a separatory funnel. The mixture was washed with brine and the organic phase was dried over anhydrous Na_2SO_4, filtered and evaporated under reduced pressure to afford a yellow solid. The crude was purified via flash column chromatography (100% DCM to 8:2 DCM/MeOH) to afford a white solid. (252 mg, 73%)

MS (ESI+), m/z 402.2

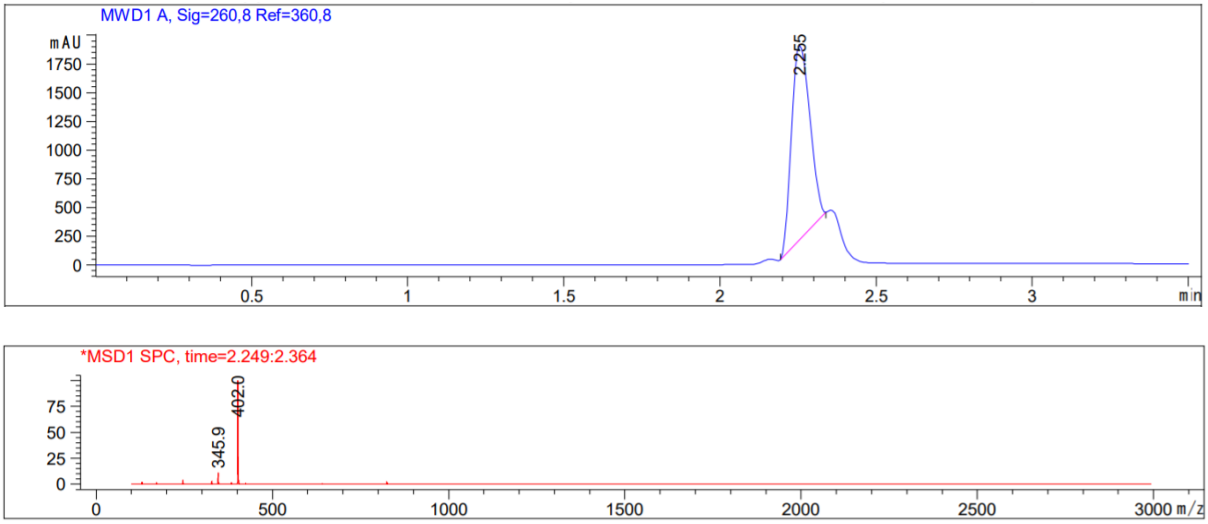

Synthesis of negOncoFAP-Asp-Lys-Asp-Cys (18)

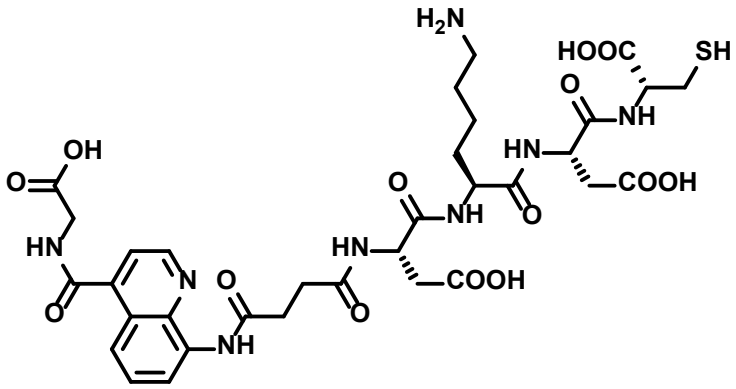

To a solid-phase synthesis syringe, H-Cys(Trt)-2-CT-polystyrene resin (150 mg) was added and then swollen with DMF for 15 min. Fmoc-L-Asp(OtBu)-OH (72 mg, 0.18 mmol, 2 eq.), HATU (67 mg, 0.18 mmol, 2 eq.) and DIPEA (46 µL, 0.36 mmol, 4 eq.) were sequentially added to the resin. The mixture was allowed to react for 2 h, then treated with a 20% solution of Piperidine in DMF (3 mL) for the Fmoc-removal and washed several times with DMF. The resin was then treated with a solution of Fmoc-L-Lys(Boc)-OH (82 mg, 0.18 mmol, 2 eq.), HATU (67 mg, 0.18 mmol, 2 eq.) and DIPEA (46 µL, 0.36 mmol, 4 eq.) in DMF (3 mL) for 2 h, following Fmoc-removal with a 20% solution of Piperidine in DMF (3 mL). After washing with DMF, a solution of Fmoc-L-Asp(OtBu)-OH (72 mg, 0.18 mmol, 2 eq.), HATU (67 mg, 0.18 mmol, 2 eq.) and DIPEA (46 µL, 0.36 mmol, 4 eq.) in DMF (3 mL) was added to the resin. After 1 h, the resin was washed and treated with a 20% solution of Piperidine in DMF (3 mL). Lastly, the resin was treated with a solution of negOncoFAP-COOH (72 mg, 0.18 mmol, 2 eq.), HATU (67 mg, 0.18 mmol, 2 eq.) and DIPEA (46 µL, 0.36 mmol, 4 eq.) in DMF (5 mL) for 2 h. The peptide was then cleaved from the resin using 5 mL of a solution of TFA/Triisopropylsilane/Thioanisol/water in DCM (30 : 5 : 2.5 : 2.5 : 60) for 1 h. The residue was concentrated under *vacuum*, resuspended in cold diethyl ether and centrifugated. The supernatant was discarded, and the pellet was dissolved in DMF and purified via RP-HPLC using a gradient of Water/ACN + 0.1% TFA in 7 min. The desired fractions were collected and lyophilized to afford a white solid. (18 mg, 25%).

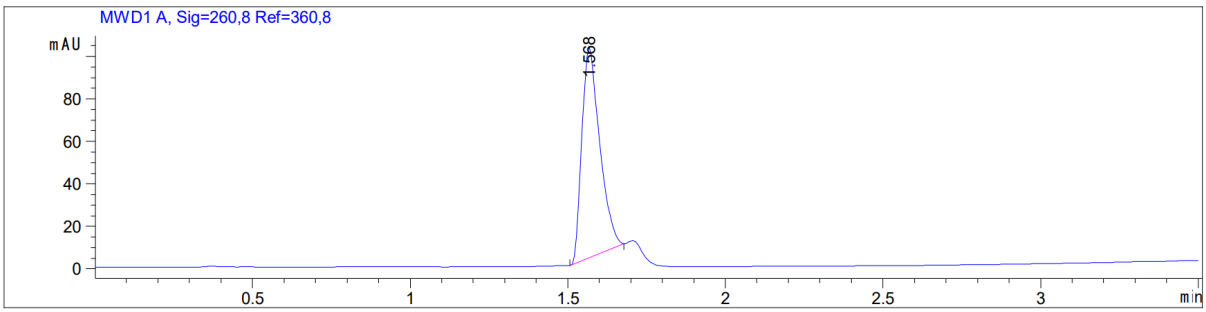
MWD1 A, Sig=260,8 Ref=360,8
mAU
1.568
0
20
40
60
80
0.5
1
1.5
2
2.5
3
min

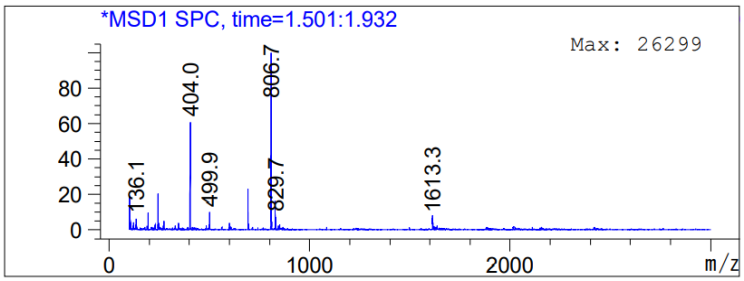
*MSD1 SPC, time=1.501:1.932
Max: 26299
136.1
404.0
499.9
806.7
829.7
1613.3
0
20
40
60
80
0
1000
2000
m/z

Synthesis of negOncoFAP-Alexa488 (19)

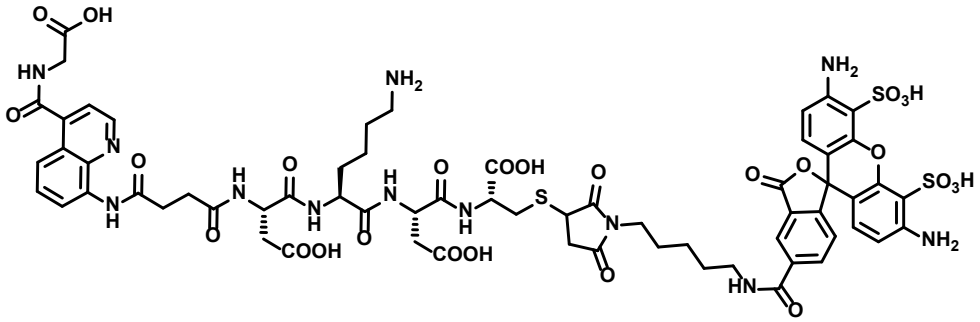

negOncoFAP-Asp-Lys-Asp-Cys (compound **18**, 1.0 mg, 0.6 µmol, 1.0 eq) is dissolved in PBS pH 7.4 (300 µL). Alexa FluorTM 15 488 C5 Maleimide (200 µg, 0.3 µmol, 0.5 eq) is added as dry DMSO solution (200 µL). The reaction is stirred for 3 h. The crude material is purified by RP-HPLC (Water 0.1% TFA/ACN 0.1%TFA 95:5 to 2:8 in 20 min) and lyophilized, to obtain an orange solid. (0.9 mg, 72%)

MS(ES+), m/z 1505.2

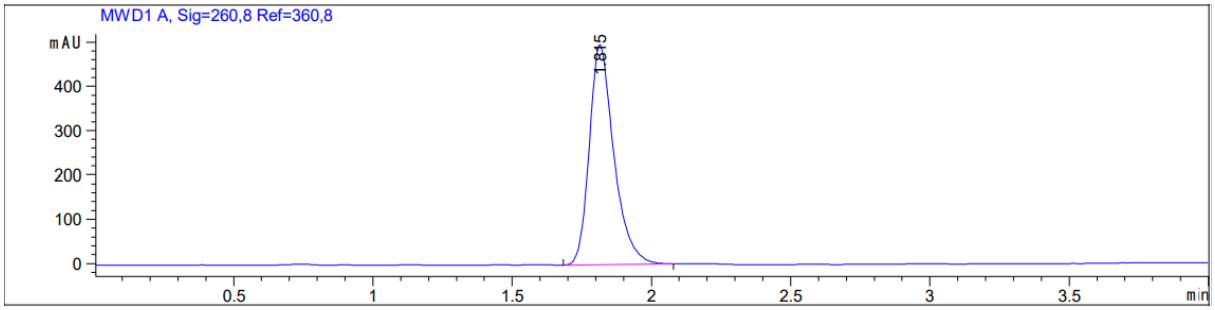

Synthesis of negBiOncoFAP-Asp-Lys-Asp-Cys (20)

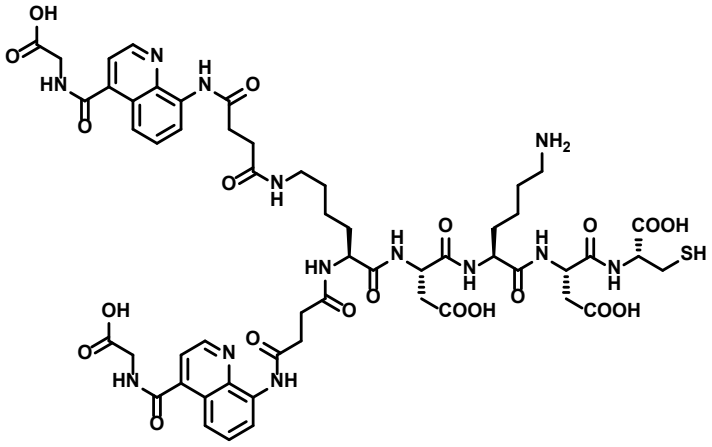

To a solid-phase synthesis syringe, H-Cys(Trt)-2-CT-polystyrene resin (250 mg) was added and then swollen with DMF for 15 min. Fmoc-L-Asp(OtBu)-OH (123 mg, 0.3 mmol, 2 eq.), HATU (114 mg, 0.3 mmol, 2 eq.) and DIPEA (105 µL, 0.6 mmol, 4 eq.) were sequentially added to the resin. The mixture was allowed to react for 2 h, then treated with a 20% solution of Piperidine in DMF (3 mL) for the Fmoc-removal and washed several times with DMF. The resin was then treated with a solution of Fmoc-L-Lys(Boc)-OH (140 mg, 0.3 mmol, 2 eq.), HATU (114 mg, 0.3 mmol, 2 eq.) and DIPEA (105 µL, 0.6 mmol, 4 eq.) in DMF (3 mL) for 2 h, following Fmoc-removal with a 20% solution of Piperidine in DMF (3 mL). After washing with DMF, a solution of Fmoc-L-Asp(OtBu)-OH (123 mg, 0.3 mmol, 2 eq.), HATU (114 mg, 0.3 mmol, 2 eq.) and DIPEA (105 µL, 0.6 mmol, 4 eq.) in DMF (3 mL) was added to the resin. After 1 h, the resin was washed and treated with a 20% solution of Piperidine in DMF (3 mL). Subsequently, Fmoc-L-Lys(Fmoc)-OH (180 mg, 0.3 mmol, 2 eq.), HATU (114 mg, 0.3 mmol, 2 eq.) and DIPEA (105 µL, 0.6 mmol, 4 eq.) and DMF (3 mL) were added to the resin and the mixture was allowed to react for 2 h, following Fmoc-removal with 20% solution of Piperidine in DMF (3 mL). Lastly, the resin was treated with a solution of negOncoFAP-COOH (240 mg, 0.6 mmol, 4 eq.), HATU (228 mg, 0.6 mmol, 4 eq.) and DIPEA (155 µL, 1.20 mmol, 8 eq.) in DMF (15 mL) for 2 h. The peptide was then cleaved from the resin using 5 mL of a solution of TFA/Triisopropylsilane/Thioanisol/water in DCM (30 : 5 : 2.5 : 2.5 : 60) for 1 h. The residue was concentrated under vacuo, resuspended in cold diethyl ether and centrifugated. The supernatant was discarded, and the pellet was dissolved in DMF and purified via RP-HPLC using a gradient of water/ACN + 0.1% TFA in 7 min. The desired fractions were collected and lyophilized to afford a white solid. (24 mg, 13%)

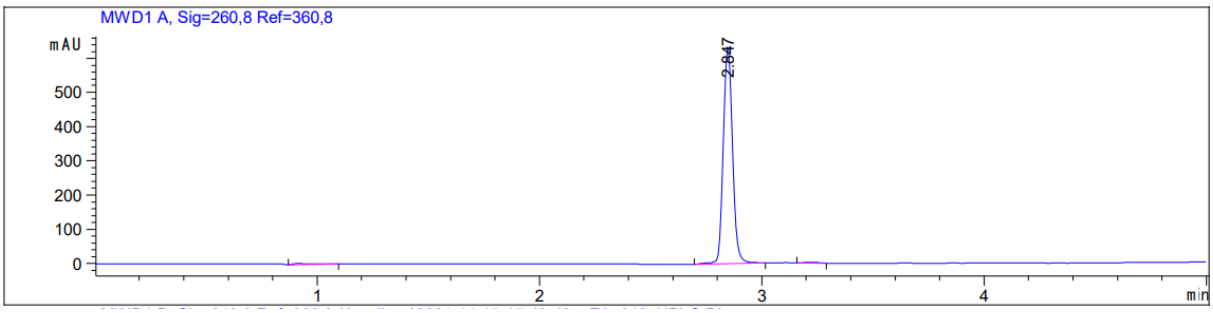
MWD1 A, Sig=260,8 Ref=360,8
mAU
500
400
300
200
100
0
2.847
1
2
3
4
min

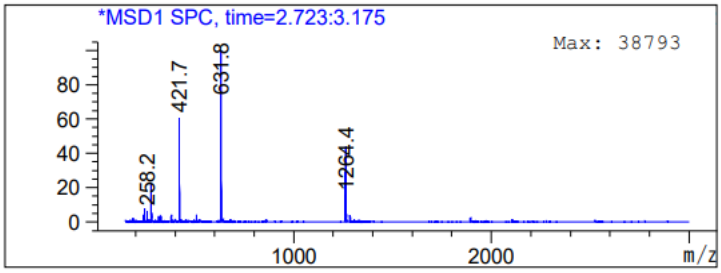
*MSD1 SPC, time=2.723:3.175
Max: 38793
80
60
40
20
0
258.2
421.7
631.8
1264.4
1000
2000
m/z

Synthesis of negBiOncoFAP-Alexa488 (21)

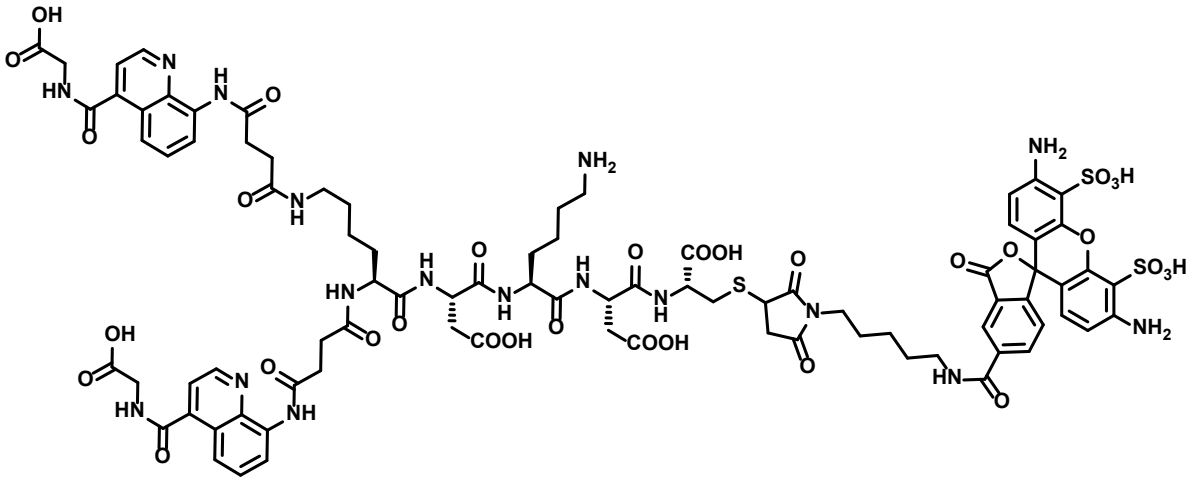

negBiOncoFAP-Asp-Lys-Asp-Cys (compound **22**) (1 mg, 0.59 µmol, 1.0 eq) is dissolved in PBS pH 7.4 (300 µL). Alexa FluorTM 15 488 C5 Maleimide (200 µg, 0.29 µmol, 0.5 eq) is added as dry DMSO solution (200 µL). The reaction is stirred for 3 h. The crude material is purified by RP-HPLC (Water 0.1% TFA/ACN 0.1%TFA 9.5:0.5 to 2:8 in 20 min) and lyophilized, to obtain an orange solid. (0.9 mg, 59%)

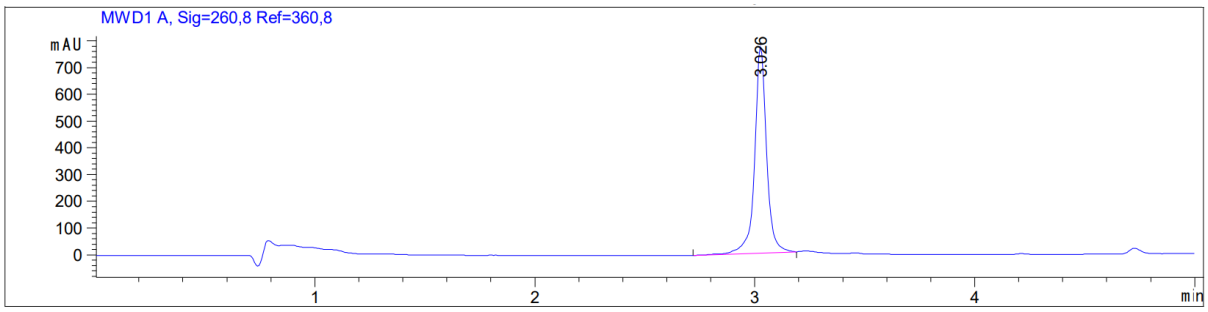

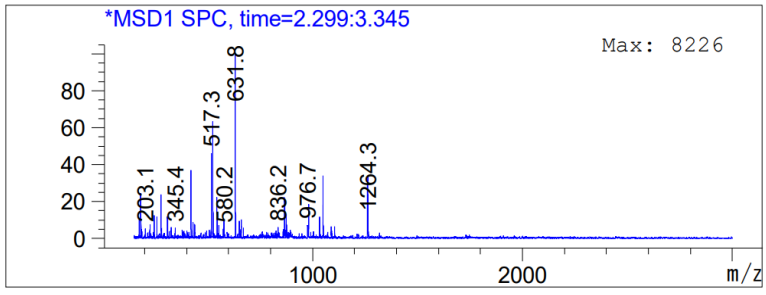

Quality Control of Radiosynthesis – Radio-HPLC

Reversed-phase Radio-HPLC were performed on a Merck-Hitachi D-7000 Series equipped with Raytest GABI-Star radio detector, using a Synergi 4 µm Polar-RP 80 Å, 150 x 4.6 mm column at a flow rate of 1 ml min-1 with linear gradients of solvents Millipore water and CAN.

Quality Control of Radiosynthesis - Coelution Experiments of Ligand–Protein Complexes.

PD-10 columns were pre-equilibrated with running buffer (50 mM Tris, 100 mM NaCl, pH = 7.4). 150 µL of a solution containing hFAP (2 µM) or hCAIX (irrelevant protein, 2 µM) was pre-incubated with 2 µL of ^{177}Lu-OncoFAP or ^{177}Lu-BiOncoFAP stock solution (50 µM, 5 MBq). The final solution was loaded on the column and flushed with running buffer. Fractions of the flow-through (200 µL) were collected in test tubes and the radioactivity measured with a Packard Cobra γ-counter. As negative control, 2 µL of ^{177}Lu-OncoFAP or ^{177}Lu-BiOncoFAP stock solution (50 µM, 5 MBq) were diluted in 150 µL of running buffer (50 mM Tris, 100 mM NaCl, pH = 7.4), without proteins. The final solution was loaded on the column and flushed with running buffer. Fractions of the flow-through (200 µL) were collected in test tubes and the radioactivity measured with a Packard Cobra γ-counter. Results of the co-elution experiments performed with ^{177}Lu-OncoFAP and ^{177}Lu-BiOncOFAP on hFAP, hCAIX (irrelevant protein) and without protein are shown in Figure S1.

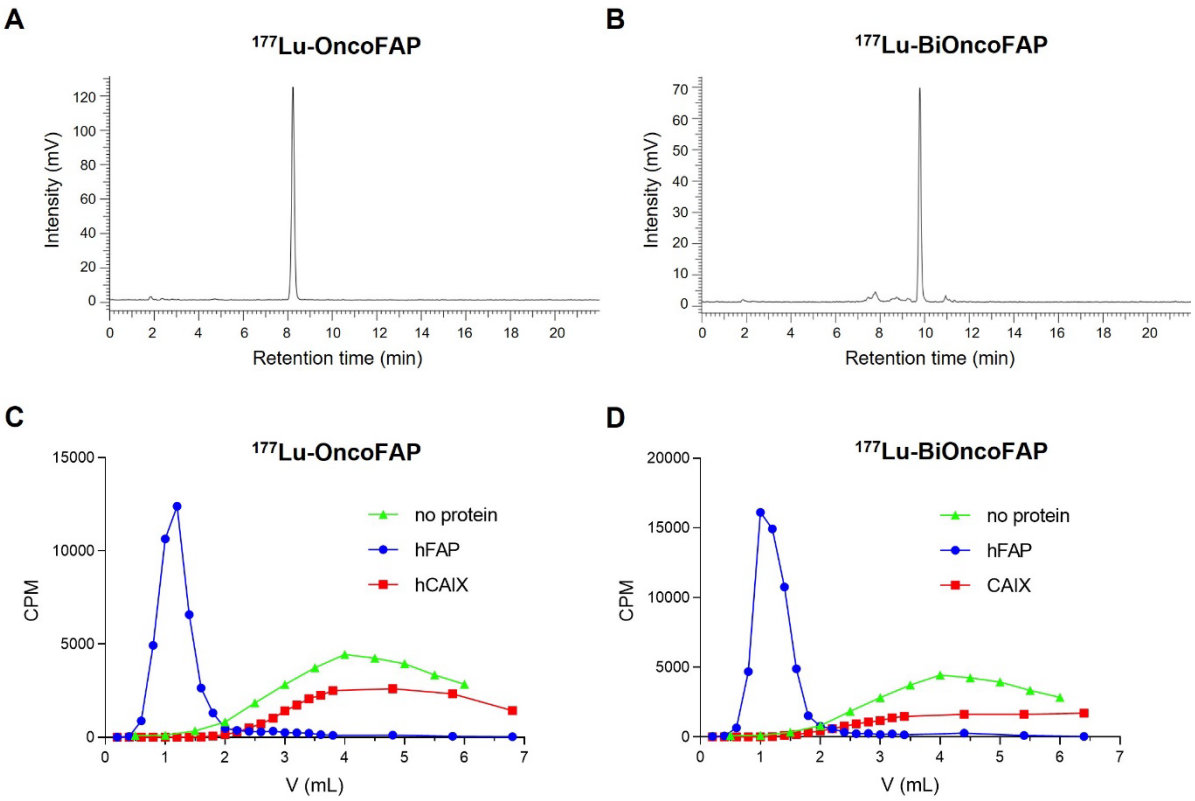

Supplemental Figure 1. Quality control of radiosynthesis. Radio-HPLC of ^{177}Lu-OncoFAP (*A*) and ^{177}Lu-BiOncoFAP (*B*); PD-10 experiments of ^{177}Lu-OncoFAP (*C*) and ^{177}Lu-BiOncoFAP (D) incubated with hFAP, using no protein or irrelevant protein (hCAIX) as a negative control.

IN VITRO TESTS AND ASSAYS

Affinity Measurement to Non-Target Proteins by Fluorescence Polarization.

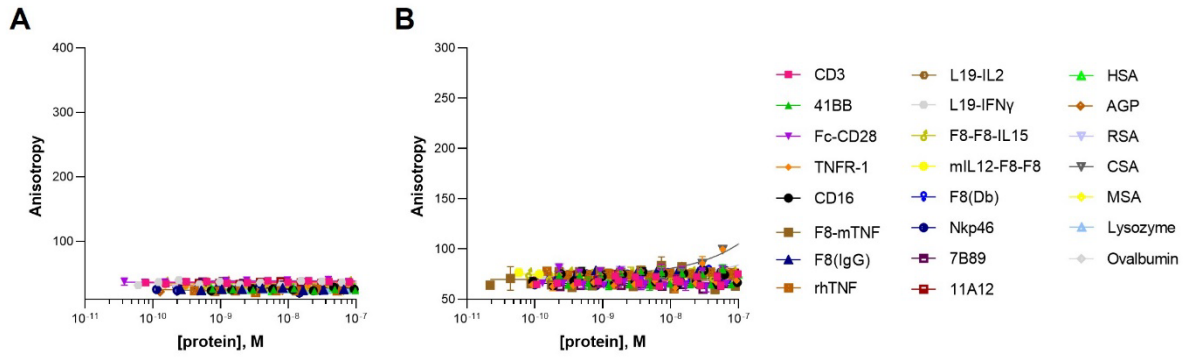

Supplemental Figure 2. Fluorescence polarization experiments of OncoFAP-Fluorescein (*A*) and BiOncoFAP-Fluorescein (*B*) towards a panel of non-target proteins, including tumour-associated antigens, abundant proteins and irrelevant proteins.

Stability in Human and Mouse Blood Serum.

36 µL of serum (either mouse “Sigma Aldrich”, human “Sigma Aldrich”) were preincubated at 37 °C for 5 minutes. 4 µL of a 1 mM DMSO solution of the analytes was added at the final concentration of 50 µM to start the kinetic. The assay was blocked by deproteinization with 300 µL of ACN at 0, 24, 48, 72 and 120 hours after the addition of the compound. Deproteinized samples were centrifugated at 14000 g for 10 minutes. 200 µL of supernatant was dried under vacuum at 37 °C and carefully resuspended in 30 µL of an aqueous solution containing 10% ACN and 0.1 % HCOOH. Samples were analyzed via LC-MS. Chromatographic separation was carried out on an Agilent 1200 Series LC System using as column an InfinityLab Poroshell 120 EC-C18, (4.6 x 56 mm) at a flow rate of 0.8 mL/min with linear gradients of solvents A and B (A = Millipore water with 0.1% formic acid, B = ACN with 0.1% formic acid) from 40% to 100% of B in 3 minutes. Eluents were analyzed in full mass scan in positive ion mode with an Agilent 6100 Series Single Quadrupole MS 5 System.

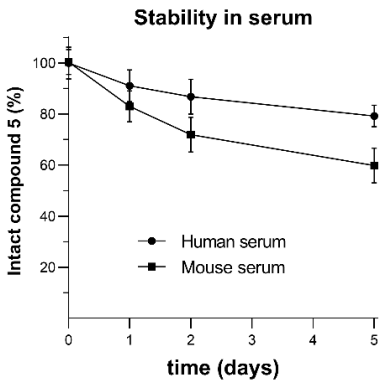

Supplemental Figure 3. *In vitro* stability of [^{nat}Lu]Lu-BiOncoFAP-DOTAGA (**5**) in human and mouse serum at 37°C, 50 µM over time.

Determination of Log$D_{7.4}$ values of ^{177}Lu-OncoFAP and ^{177}Lu-BioncoFAP.

The lipophilicity of ^{177}Lu-OncoFAP and ^{177}Lu-BiOncoFAP was determined as follows. 100 µL aliquotes of the radioligand (~ 1 MBq) in PBS buffer were added to PBS buffer (500 µL, pH 7.4) and 1-octanol (600 µL). The two-layer mixture were vigorously shaken for 10 minutes on a vortex mixer and then centrifuged at 700 rpm for 5 min to facilitate the separation. 100 µL aliquotes of both layers were measured in a Packard Cobra Gamma Counter and the partition coefficient was determined by dividing cpm (octanol) by cpm (PBS) and indicated as Log$D_{7.4}$.

Log$D_{7.4}$ (^{177}Lu-OncoFAP): -4.02

Log$D_{7.4}$ (^{177}Lu-BiOncoFAP): -3.60

ANIMAL STUDIES

In vivo Tumour and Organ Penetration Analysis of OncoFAP and BiOncoFAP.

SK-RC-52.hFAP and SK-RC-52.wt xenografted tumours were implanted respectively into the right and left flank of female athymic Balb/c AnNRj-Foxn1 mice (6-8 weeks of age) as described above, and allowed to grow to an average volume of 200 mm^3.

OncoFAP-IRDye750 (compound **11**) and BiOncoFAP-IRDye750 (compound **12**) were administered intravenously at a dose of 250 nmol/kg.

Fluorescence images were aquired at different time points (10 min, 1 h, 2 h, 3 h, 4.5 h, 6 h) on an IVIS Spectrum imaging system (Xenogen, exposure 1s, binning factor 8, excitation at 745 nm, emission filter at 800 nm, f number 2, field of view 13.1). Six hours after administration, mice were euthanized by CO_2 asphyxiation. Tumours, organs and blood were collected, and fluorescence images acquired as described above.

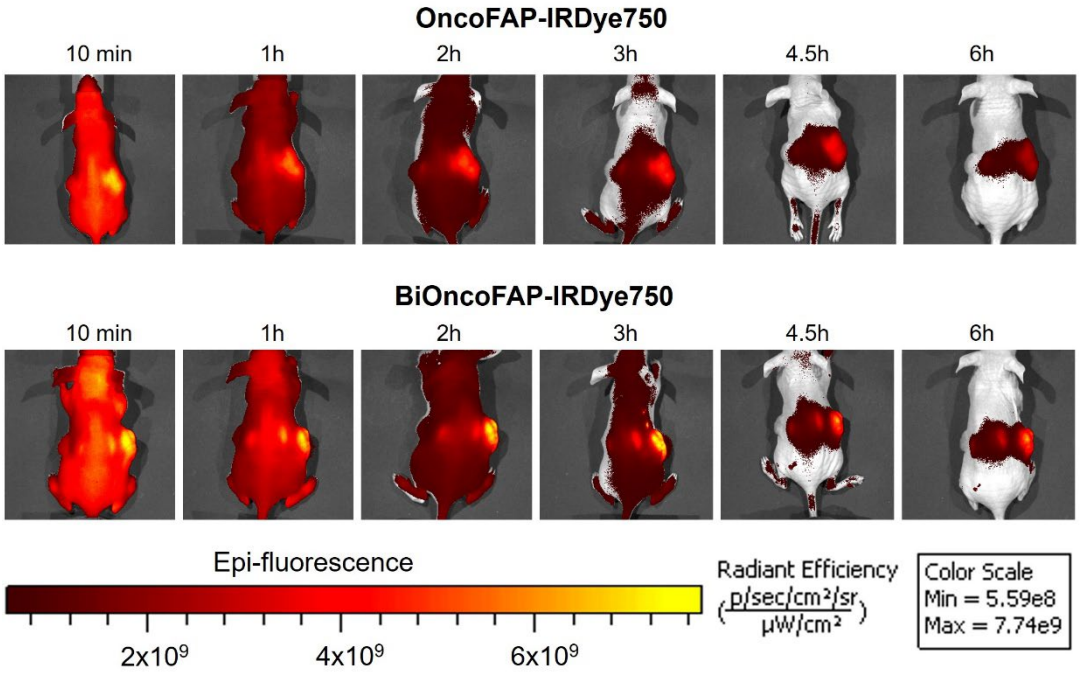

Supplemental Figure 4. Near-infrared fluorescence imaging evaluation of the targeting performance of OncoFAP-IRDye750 and BiOncoFAP-IRDye in mice bearing SK-RC-52.hFAP tumours (right flank) and SK-

RC-52.wt tumours (left flank). Images were collected at different time points (10 min, 1 h, 2 h, 3 h, 4.5 h, 6 h) after the intravenous injection (250 nmol/kg).

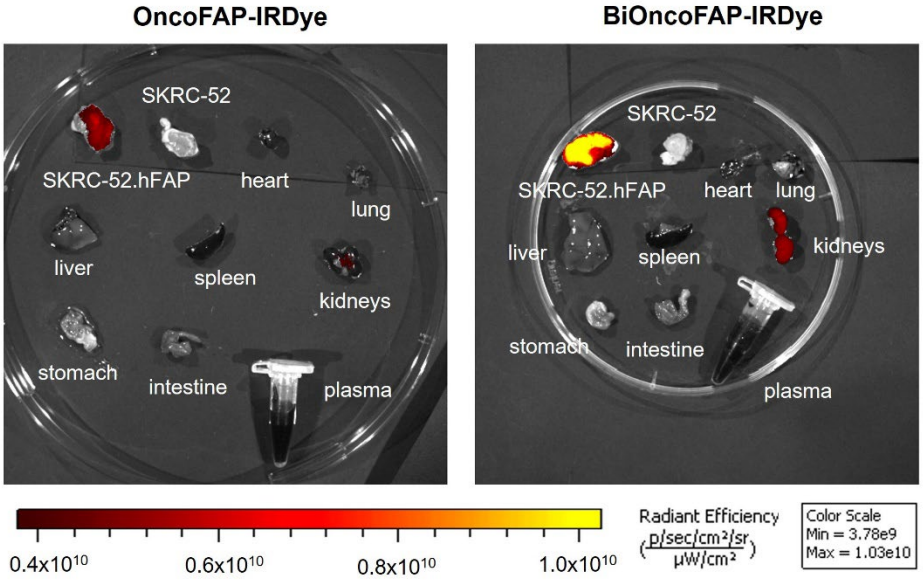

Supplemental Figure 5**.** Near-infrared fluorescence imaging evaluation of the targeting performance of OncoFAP-IRDye750 and BiOncoFAP-IRDye in mice bearing SK-RC-52.hFAP tumours (right flank) and SK-RC-52.wt tumours (left flank). Mice were euthanized 6 h after systemic administration (250 nmol/kg) and images were collected.

Quantitative Biodistribution of ^{177}Lu-OncoFAP and ^{177}Lu-BiOncoFAP in Tumour-Bearing Mice.

Supplemental Table 1. Quantitative in vivo biodistribution of ^{177}Lu-OncoFAP at different time points after intravenous administration (250 nmol/kg, 50 MBq/kg) in mice bearing HT-1080.wt and HT-1080.hFAP tumours. Data are reported as %ID/g ± standard deviation (n = 4 or 5).

	^{177}Lu-OncoFAP (%ID/g)			
	1 h	**4 h**	**17 h**	**24 h**
Tumor (hFAP)	18.69 ± 3.54	19.02 ± 5.69	6.37 ± 0.74	4.41 ± 0.65
Tumor (wt)	0.53 ± 0.06	0.71 ± 0.11	0.24 ± 0.12	0.39 ± 0.21
Liver	3.25 ± 0.88	0.84 ± 0.22	0.14 ± 0.04	0.11 ± 0.03
Lung	0.49 ± 0.06	0.21 ± 0.07	0.06 ± 0.07	0.03 ± 0.01
Spleen	0.17 ± 0.02	0.11 ± 0.04	0.02 ± 0.00	0.03 ± 0.03
Hearth	0.14 ± 0.01	0.09 ± 0.02	0.02 ± 0.01	0.25 ± 0.50
Kidney	2.06 ± 0.45	2.20 ± 0.48	1.01 ± 0.31	0.64 ± 0.43
Intestine	0.74 ± 0.38	0.50 ± 0.23	0.04 ± 0.02	0.13 ± 0.20
Tail	0.66 ± 0.31	2.79 ± 2.06	2.02 ± 1.33	0.32 ± 0.20
Blood	0.49 ± 0.20	0.18 ± 0.09	0.04 ± 0.03	0.01 ± 0.01

Supplemental Table 2. Tumor-to-organ ratios of ^{177}Lu-OncoFAP at different time points after intravenous administration (250 nmol/kg, 50 MBq/kg) in mice bearing HT-1080.wt and HT-1080.hFAP tumours. Data are reported as tumor:organ ratio ± standard deviation (n = 4 or 5).

	^{177}Lu-OncoFAP (tumor-to-organ ratio)			
	1 h	**4 h**	**17 h**	**24 h**
Tumor (wt)	35.84 ± 2.50	26.80 ± 6.42	32.63 ± 17.40	13.29 ± 5.95
Liver	5.50 ± 0.29	22.57 ± 3.13	48.22 ± 15.89	38.84 ± 8.58
Lung	39.14 ± 1.05	94.52 ± 30.66	179.36 ± 106.03	178.73 ± 106.16
Spleen	109.03 ± 10.95	176.69 ± 70.98	240.04 ± 54.72	132.06 ± 85.32
Hearth	144.28 ± 4.15	217.83 ± 118.73	424.12 ± 276.86	215.54 ± 219.63
Kidney	9.13 ± 1.07	8.63 ± 1.522	6.86 ± 2.44	15.22 ± 20.46
Intestine	49.55 ± 46.78	41.64 ± 11.90	194.70 ± 113.64	98.46 ± 75.01
Tail	29.02 ± 8.80	10.84 ± 7.95	5.68 ± 6.12	11.21 ± 2.94
Blood	51.54 ± 4.59	118.15 ± 52.11	282.15 ± 227.142	1139.61 ± 395.66

Supplemental Table 3. Quantitative in vivo biodistribution of ^{177}Lu-BiOncoFAP at different time points after intravenous administration (250 nmol/kg, 50 MBq/kg) in mice bearing HT-1080.wt and HT-1080.hFAP tumours. Data are reported as %ID/g ± standard deviation (n = 4 or 5).

	^{177}Lu-BiOncoFAP (%ID/g)				
	1 h	**4 h**	**17 h**	**24 h**	**48 h**
Tumor (hFAP)	28.95 ± 5.21	31.18 ± 3.70	19.99 ± 4.34	19.21 ± 5.42	16.46 ± 3.18
Tumor (wt)	1.33 ± 0.34	1.11 ± 0.15	0.79 ± 0.19	0.72 ± 0.17	0.33 ± 0.04
Liver	1.60 ± 0.43	0.93 ± 0.11	0.56 ± 0.12	0.55 ± 0.02	0.23 ± 0.01
Lung	1.52 ± 0.43	0.42 ± 0.06	0.18 ± 0.09	0.17 ± 0.02	0.04 ± 0.01
Spleen	0.82 ± 0.48	0.35 ± 0.08	0.24 ± 0.07	0.21 ± 0.06	0.15 ± 0.07
Hearth	0.56 ± 0.06	0.22 ± 0.04	0.11 ± 0.02	0.08 ± 0.01	0.04 ± 0.03
Kidney	4.27 ± 1.51	3.21 ± 0.25	2.09 ± 0.52	1.61 ± 0.27	0.75 ± 0.17
Intestine	0.48 ± 0.04	0.36 ± 0.18	0.16 ± 0.06	0.16 ± 0.10	0.06 ± 0.02
Tail	2.83 ± 0.79	2.93 ± 1.30	1.34 ± 0.44	1.24 ± 0.32	0.22 ± 0.06
Blood	0.92 ± 0.23	0.47 ± 0.07	0.17 ± 0.05	0.10 ± 0.02	0.02 ± 0.02

Supplemental Table 4. Tumor-to-organ ratios of ^{177}Lu-BiOncoFAP at different time points after intravenous administration (250 nmol/kg, 50 MBq/kg) in mice bearing HT-1080.wt and HT-1080.hFAP tumours. Data are reported as tumor:organ ratio ± standard deviation (n = 4 or 5).

	^{177}Lu-BiOncoFAP (tumor-to-organ ratios)				
	1 h	**4 h**	**17 h**	**24 h**	**48 h**
Tumor (wt)	22.99 ± 8.09	28.64 ± 7.34	26.66 ± 9.32	28.00 ± 11.02	50.38 ± 12.01
Liver	18.76 ± 5.31	33.82 ± 6.19	35.92 ± 5.58	34.44 ± 9.69	70.53 ± 16.52
Lung	19.54 ± 4.09	75.62 ± 16.76	136.84 ± 76.67	111.94 ± 26.04	443.90 ± 155.8
Spleen	42.09 ± 17.74	94.61 ± 35.77	86.03 ± 14.36	101.25 ± 63.64	121.56 ± 64.44
Hearth	52.23 ± 10.83	143.74 ± 29.62	188.61 ± 26.39	230.93 ± 71.07	539.71 ± 352.4
Kidney	7.19 ± 2.29	9.77 ± 1.69	9.67 ± 1.50	11.85 ± 2.42	22.42 ± 5.55
Intestine	59.58 ± 6.48	98.77 ± 36.64	130.41 ± 31.78	134.80 ± 55.74	288.07 ± 137.5
Tail	10.43 ± 1.72	12.40 ± 5.75	16.52 ± 7.92	16.86 ± 8.38	82.85 ± 47.37
Blood	32.75 ± 8.97	67.21 ± 10.01	119.46 ± 21.39	196.24 ± 72.98	1270.2 ± 138.1

In vitro Cell Binding and Efflux Assays

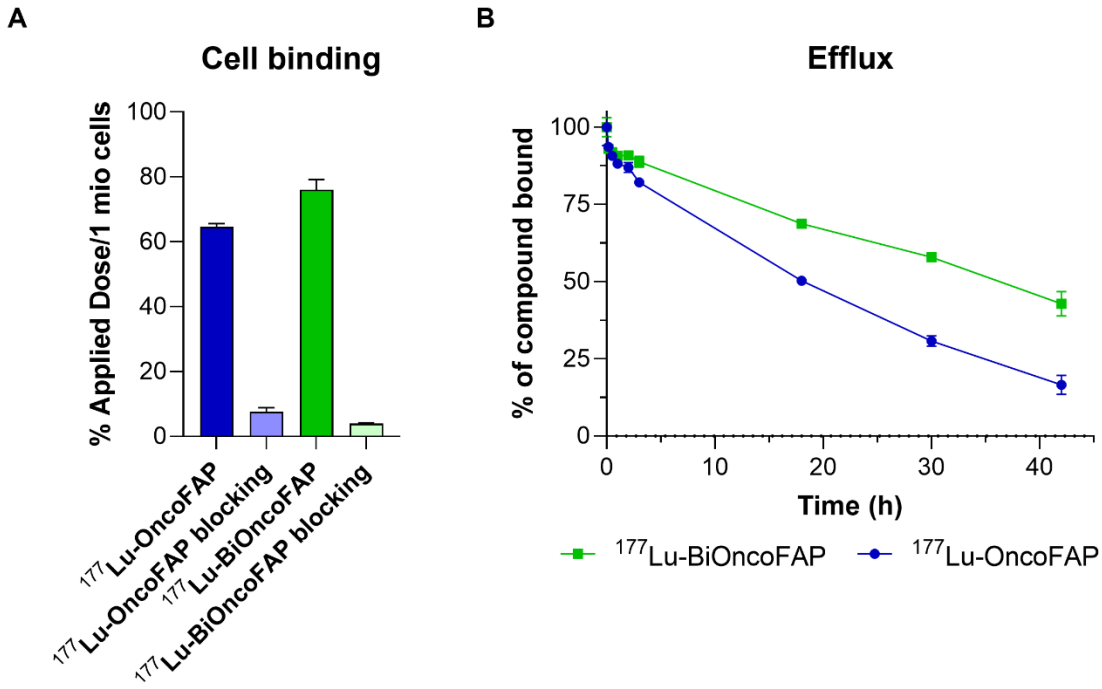

Supplemental Figure 6. *In vitro* cell binding (*A*) and efflux (*B*)

HT-1080.hFAP cells, were cultured using DMEM medium (Gibco) supplemented with 10% Fetal Bovine Serum (FBS, Gibco) and 1% Antibiotic-Antimytotic (Gibco). Cells were seeded in 24-well plates (0.2 mln cells/well, 0.5 mL/well) and incubated overnight at 37°C, 5% CO_2. Then, media was removed, cells were washed with PBS (2 x 0.5 mL) and incubated with a solution of ^{177}Lu-OncoFAP or ^{177}Lu-BiOncoFAP (10 KBq, 1 pmol, 0.5 mL). For the competitive binding experiments, a 1'000'000-fold excess of cold competitors was added to the media.

Cell binding

After 1 h incubation, cells were washed in PBS, lysed with a 1M NaOH, 2% SDS solution (0.5 mL), and fractions of the resulting suspension were measured with a gamma counter (Packard Cobra). Radioactivity was calculated as percentage of the applied dose per million cells.

Efflux

Fractions of the culture media were measured with a gamma counter (Packard Cobra) at different time-points. Percentage of compound bound was calculated as fraction of the total activity and corrected for the ^{177}Lu decay.

Single Mouse Tumor Growth Values in Therapy Studies

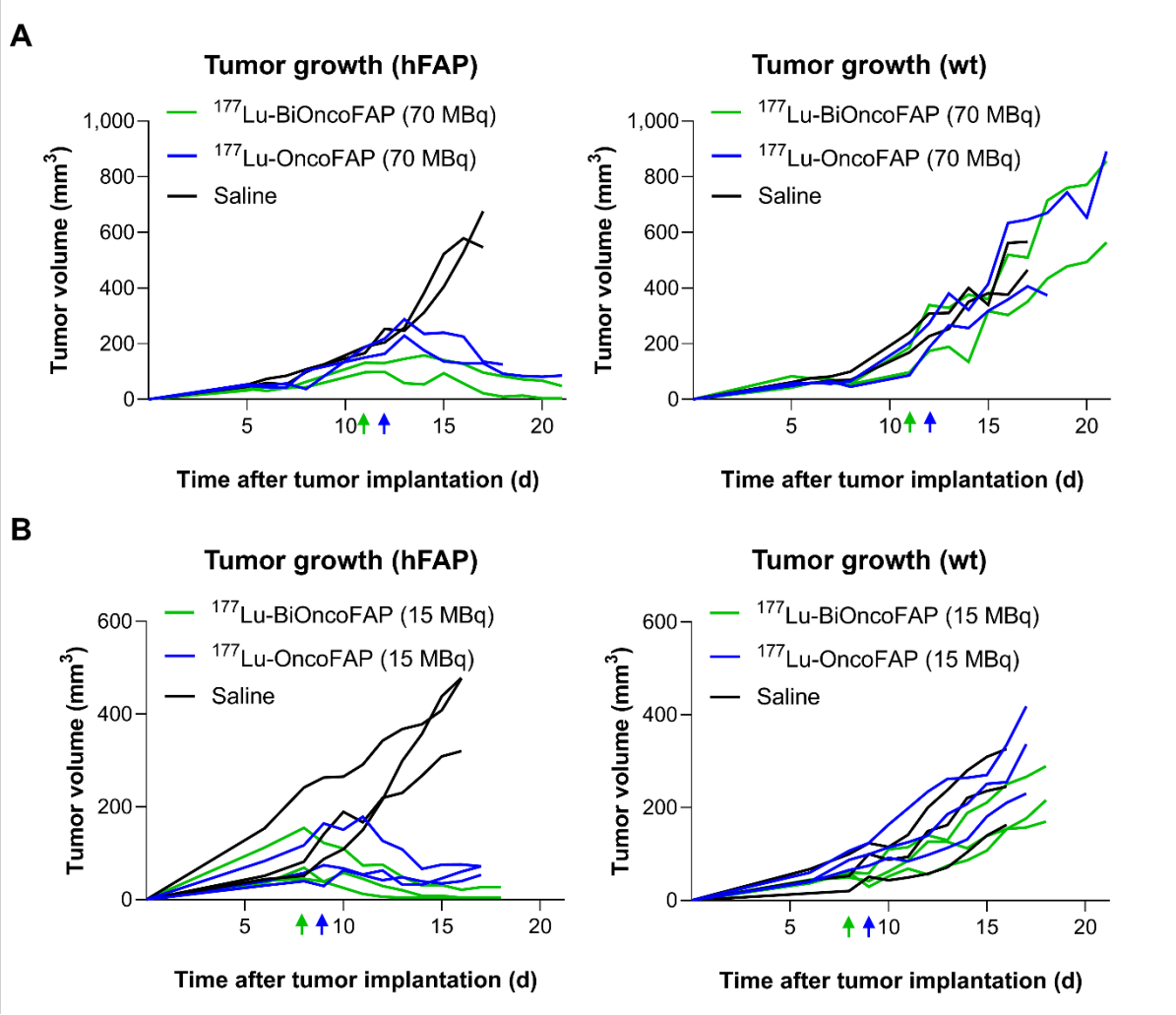

Supplemental Figure 7. Therapeutic activity after a single administration (250 nmol/kg) of ^{177}Lu-OncoFAP (compound **3**) and ^{177}Lu-BiOncoFAP (compound **6**) in Balb/c nu/nu mice bearing HT-1080.hFAP tumour in the right flank and HT-1080.wt tumour in the left flank at a dose of (*A*) 70 MBq/mouse or (*B*) 15 MBq/mouse. The efficacy of the different treatments was assessed by daily measurement of tumour volume (mm^3) after administration of the different compounds. Data represent single mouse tumour volume.

Body Weight Change in Therapy Studies

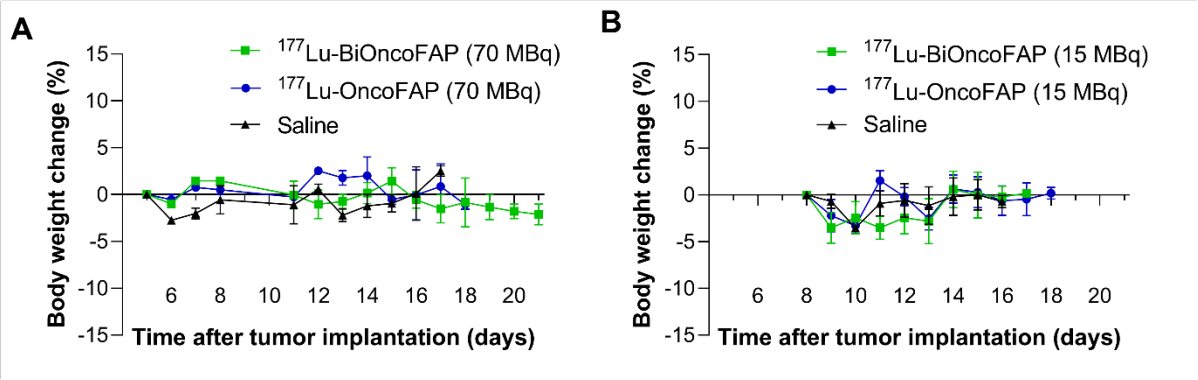

Supplemental Figure 8**.** Percentage of Body weight change was assessed daily in therapy studies at (*A*) 70 MBq/mouse and (*B*) 15 MBq/mouse doses.